

THERMAL EFFECTS IN THE PARAMETRIC EXCITATION
OF THIN PLATES

A THESIS

Presented to

The Faculty of the Division of Graduate
Studies and Research

By

Parthasarathi Mukhopadhyay

In Partial Fulfillment
of the Requirements for the Degree
Doctor of Philosophy
in the School of Aerospace Engineering

Georgia Institute of Technology

May 1975

THERMAL EFFECTS IN THE PARAMETRIC EXCITATION
OF THIN PLATES

Approved:

R. L. Carlson, Chairman

J. I. Craig

W. W. King

Date approved by Chairman: 5-19-75

ACKNOWLEDGMENTS

The author wishes to express his profound gratitude to his advisor, Dr. R. L. Carlson, for his valuable guidance and many hours of very illuminating discussions.

He would also like to thank Drs. J. I. Craig, W. W. King, D. J. McGill, and G. A. Pierce, for their constructive criticism and valuable suggestions.

Further acknowledgments are due to the School of Aerospace Engineering for the award of a research assistantship.

Special thanks go to Mr. R. B. Deo, a good friend, for his help in the preparation of the final manuscript.

TABLE OF CONTENTS

	Page
ACKNOWLEDGMENTS	ii
LIST OF TABLES	v
LIST OF ILLUSTRATIONS	vi
SUMMARY.	vii
Chapter	
I. INTRODUCTION	1
Dynamic Stability	
Thermal Effects	
Historical Background	
Objective	
II. GOVERNING EQUATIONS	6
Introduction	
Strain Displacement Relation	
Stress-Strain Equations	
Equations of Motion	
III. DETERMINATION OF REGIONS OF INSTABILITY	25
Introduction	
Form of Solutions	
Stability of Motion	
IV. EQUATIONS OF MOTION FOR A CIRCULAR AND A RECTANGULAR PLATE.	37
Introduction	
Circular Plate	
Rectangular Plate	
V. PRESENTATION AND DISCUSSION OF RESULTS.	55
Introduction	
Computational Procedure	
Presentation of Results	
Discussion of Results	

Chapter	Page
VI. CONCLUSIONS AND RECOMMENDATIONS FOR FUTURE RESEARCH . .	78
Conclusions	
Recommendations for Future Research	
APPENDIX	
A. STRESS RESULTANTS AND MOMENTS IN TERMS OF STRAINS. . .	81
B. EXISTENCE OF PERIODIC SOLUTIONS.	83
C. INTEGRATION FORMULAE	86
D. ELEMENTS OF THE MATRIX E FOR RECTANGULAR PLATE. . . .	88
REFERENCES	93
VITA	96

LIST OF TABLES

Table	Page
1. Values of ζ_{cr} for $a = 0.1b$ Using $\phi_{on}(r, \theta)$	62
2. Values of $\bar{\zeta}$ for $\bar{\beta} = 0.5$ Using $\phi_{on}(r, \theta)$	62
3. Circular Plate--Upper Boundary Frequency $(\theta/\omega_{01})^2$	65
4. Circular Plate--Lower Boundary Frequency $(\theta/\omega_{01})^2$	65
5. Values of ζ_{cr} for $a/b = 1$	68
6. Values of $\bar{\zeta}$ for $\bar{\beta} = 0.5$	68
7. Rectangular Plate--Upper Boundary Frequency $(\theta/\omega_{11})^2$	71
8. Rectangular Plate--Lower Boundary Frequency $(\theta/\omega_{11})^2$	71

LIST OF ILLUSTRATIONS

Figure	Page
1. Simply Supported Rectangular Plate with Time-Dependent Load	1
2. Coordinate System.	7
3. Plate with Boundary Traction.	13
4. Sign Convention	17
5. Variation of Eigenvalues in Complex Plane.	32
6. Circular Plate with Boundary Forces and a Hot Spot.	39
7. Rectangular Plate with Boundary Forces.	48
8. Tent-Like Temperature Distribution	48
9. Critical Temperature Parameter vs. Hot Spot Radius.	61
10. Combination Buckling of Circular Plate.	63
11. First Principal Region of Instability of the Circular Plate. Excitation Frequency vs. Oscillating Load.	66
12. First Principal Region of Instability of the Circular Plate. Excitation Frequency vs. Temperature Parameter	67
13. Combination Buckling of Rectangular Plate.	69
14. First Principal Region of Instability of the Rectangular Plate. Excitation Frequency vs. Oscillating Load	72
15. First Principal Region of Instability of the Rectangular Plate. Excitation Frequency vs. Temperature Parameter	73
16. Area of Principal Region vs. Temperature Parameter.	75

SUMMARY

The purpose of this study is to investigate the effect of thermal stresses on stability of parametric excitation of thin plates. The governing equations are derived using the principle of virtual work with reference to a general orthogonal curvilinear coordinate system. An assumed modes method is used to obtain the equations of motion in terms of generalized coordinates. The method developed is applied to study the dynamic stability of a simply supported rectangular plate and a clamped circular plate. In both cases the influence of thermal stresses on the principal region of instability is examined. Solution of the axisymmetric thermal buckling problem of the circular plate is also presented.

CHAPTER I

INTRODUCTION

Dynamic Stability

It is well known that in many situations the static equilibrium configuration of a structural component becomes unstable. The most celebrated example of this phenomenon is the Euler Column. It has also been observed that if the parameter causing the loss of static stability is changed from a constant to an oscillating load, then for certain values of the amplitude and frequency of the load, a resonance type response develops. This phenomenon is called "dynamic instability" or "parametric resonance."

To illustrate a problem of dynamic stability, consider a simply-supported rectangular plate (Figure 1), loaded in its plane, along the longitudinal direction, by a uniform force per unit length $\bar{N}(t)$. If \bar{N} is time-independent, a problem in static stability is obtained. A possible choice of a time-dependent load is $\bar{N}^S + \bar{N}^D \cos \Theta t$, where \bar{N}^S and \bar{N}^D are amplitudes, Θ is frequency parameter, and t is the variable time. If the plate is perfectly flat, it may be expected to experi-

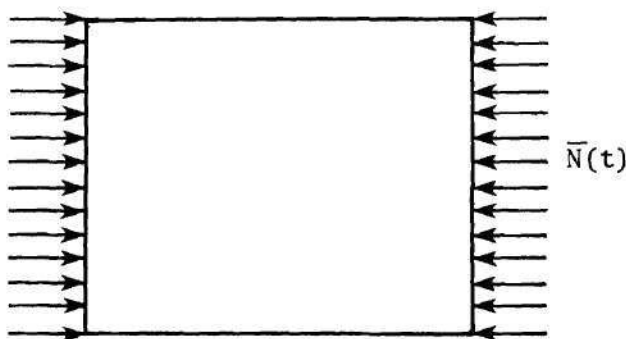


Figure 1. Simply Supported Rectangular Plate with Time-Dependent Load

ence only in-plane motion. However, a small disturbance in the direction normal to the plane of the plate can produce one of the following

responses: (1) transverse vibration with non-increasing amplitude, or (2) transverse vibration with amplitude rapidly increasing to large values. For any arbitrarily small disturbance, the motion of the plate is said to be stable in the first case, and unstable in the second. Whether the motion is stable or unstable is found to depend on the values of \bar{N}^S , \bar{N}^D , and Θ . Whether or not the motion in the second case becomes unbounded, depends on "damping" and development of the nonlinear effect of middle surface stretching.

Thermal Effects

In many engineering applications, structural components are subjected to temperature changes and gradients. Examples of such applications are found in propulsion systems which are inherently prone to high temperature effects resulting from combustion processes. In nuclear and aeronautical fields extremely high operating temperatures and gradients can occur due to the fission process and aerodynamic heating, respectively.

The problems which arise fall into three categories. The first category is associated with changes in material properties; e.g., elastic modulus and yield strength. The second category involves thermal stress. These are stresses caused by differential thermal expansions of a solid body. The last category is mainly concerned with creep. The study described here deals with the second category; i.e., thermal stress.

Historical Background

Dynamic Stability

The first mathematical analysis of a dynamic stability problem was carried out by N. M. Beliaev [1] in 1924. In the article the problem of dynamic stability of a column hinged on both ends was examined, and boundaries of the principal region of instability were determined.

R. Einaudi [2] was first to treat, in 1936, the problem of thin elastic plates loaded by periodic in-plane loads. Other pioneers in the investigation of dynamic stability of plates were V. N. Chelomei [3] and V. A. Bodner [4]. Chelomei used an energy method to solve the problem of a hinged plate that was not perfectly flat. Bodner solved a series of problems involving the dynamic stability of plates. He obtained solutions for both circular and rectangular plates. V. V. Bolotin has developed solutions to both linear and nonlinear problems of dynamic stability of plates. These appear in his book [5], The Dynamic Stability of Elastic Systems.

One of the common features of most of these works is that the equivalent static stability problem is a positive definite eigenvalue problem. Recently, R. L. Carlson [6] has reported results for an experimental investigation in which the equivalent static stability problem is neither positive nor positive definite. The paper contains photographs of test records showing the growth of amplitude when dynamic instability occurs.

A description of Russian accomplishments in the field of dynamic stability through the year 1951 is given by E. A. Beilin and G. U.

Dzhanelidze [7]. A summary of the work that has been done on the dynamic stability of columns, arches, rings, plates, and shells through the year 1965 is presented by R. M. Evan-Iwanowski [8].

Thermal Effects

The formulation of elasticity problems including the effect of temperature variation was studied by Duhamel [9] as early as 1835. Since then, a large amount of work has been done on the subject of thermal stress and excellent books on the subject [10 through 12] have been published.

Apart from altering the stress distribution caused by external loads, thermal stresses may reduce effective stiffness which, in turn, can result in an alternation of buckling and vibration behavior. Such effects of thermal stresses have been the subject of numerous studies [13, 14].

If the time-gradients of temperature are large, dynamic effects can be observed. Thermally induced vibration of beams resulting from a suddenly applied heat input was studied by B. A. Boley [15]. The dynamic response of plates was also investigated by B. A. Boley and A. D. Barber [16]. C. L. Sun and S. Y. Lu [17] have studied the non-linear, dynamic behavior of heated conical and cylindrical shells. They also investigated the stability of the resulting nonlinear vibration.

Objective

The effect of thermal stresses on the static and vibration behavior of plates has received the attention of several researchers. However, the effect of thermal stresses on the dynamic stability of

parametric excitation has remained open to research. This study aims at formulating this problem. The governing equations will be derived by application of the principle of virtual work with reference to a general orthogonal curvilinear coordinate system.

An assumed modes approach will be used to obtain the equations of motion in terms of generalized coordinates. Stability of the response will be discussed and a method for determining the boundaries of the regions of instability will be described. The method developed will be applied to study the dynamic stability of a simply supported rectangular plate and a clamped circular plate. In both cases the influence of thermal stresses on the principal regions of instability will be examined.

As limiting cases of the equations for parametric excitation, the governing equations for various other phenomena may be obtained; e.g., free vibration and thermal buckling. For the clamped circular plate problem considered here, the related thermal buckling problem has not previously been solved. This problem will be considered.

CHAPTER II

GOVERNING EQUATIONS

Introduction

In this chapter the equations governing the transverse motion of a thin plate will be derived. These equations will be specialized to forms suitable for the study of dynamic stability of problems to be considered. To begin, the terminology pertaining to plate theory will be defined.

A plate is a body bounded by two surfaces, the faces, of small curvature. The distance between these surfaces is called the thickness and it is small in comparison with the dimensions of the surface. A third bounding surface constitutes the edge of the plate, and it is cylindrical. A surface equidistant from the two faces of the plate is called the middle surface. In what follows only initially flat plates of uniform thickness and of homogeneous linear elastic material will be considered.

A right-handed orthogonal curvilinear coordinate system will be used. Let the position vector of a point in the undeformed plate be given by (see Figure 2)

$$\vec{r}(\alpha_1, \alpha_2, z) = x(\alpha_1, \alpha_2)\vec{i} + y(\alpha_1, \alpha_2)\vec{j} + z\vec{k} ,$$

where z is a coordinate normal to the middle surface of the plate. The parameters α_1 and α_2 determine the position of a point in the

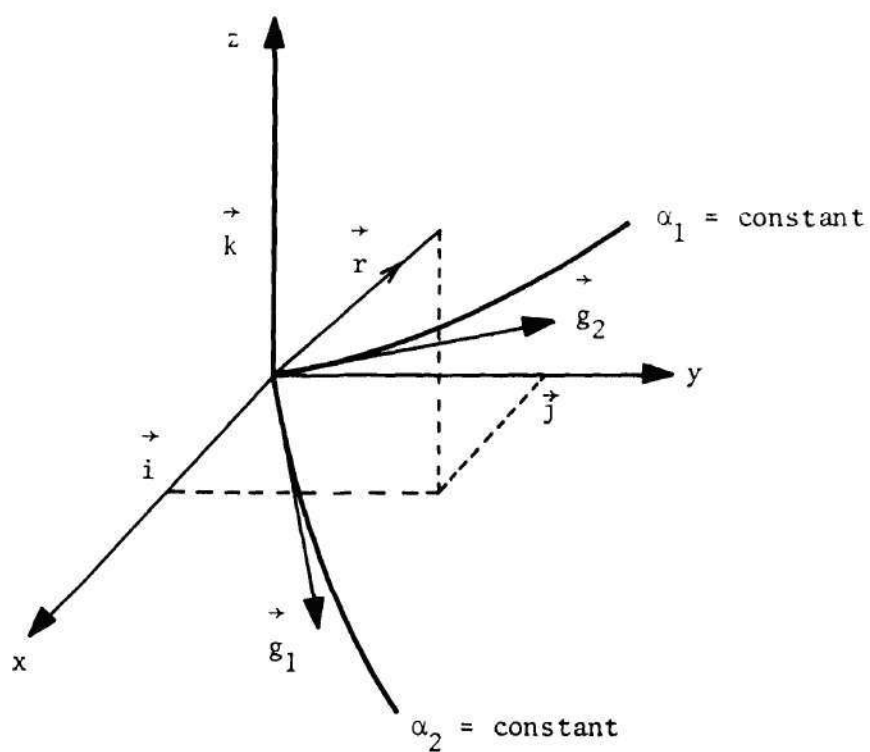


Figure 2. Coordinate System

x-y plane which coincides with middle surface. By keeping one of the parameters constant and varying the other, a family of orthogonal curves in the x-y plane is obtained. Vectors tangent to the curves along which α_2 equals a constant and α_1 equals a constant are

$$\vec{g}_1 = \frac{\partial \vec{r}}{\partial \alpha_1} \quad \text{and} \quad \vec{g}_2 = \frac{\partial \vec{r}}{\partial \alpha_2},$$

respectively. The magnitudes of these vectors are denoted by

$$G_1 = |\vec{g}_1| \quad \text{and} \quad G_2 = |\vec{g}_2|.$$

Strain Displacement Relation

Consider a point in the plate and denote its position vectors before and after deformation by $\vec{r}(\alpha_1, \alpha_2, z)$ and $\vec{r}^*(\alpha_1, \alpha_2, z)$. These are related to a displacement vector, \vec{u} , by

$$\vec{r}^* - \vec{r} = \vec{u}. \quad (1)$$

Similarly, let the position vectors of a point $(\alpha_1, \alpha_2, 0)$ of the middle surface before and after deformation be \vec{r}_0 and \vec{r}_0^* , respectively, which are related to a displacement vector \vec{u}_0 by

$$\vec{r}_0^* - \vec{r}_0 = \vec{u}_0. \quad (2)$$

Let the components of \vec{u} and \vec{u}_0 be defined as follows:

$$\vec{u} = u_1 \frac{\vec{g}_1}{G_1} + u_2 \frac{\vec{g}_2}{G_2} + u_3 \vec{k} \quad (3)$$

$$\vec{u}_0 = u \frac{\vec{g}_1}{G_1} + v \frac{\vec{g}_2}{G_2} + w \vec{k} \quad (4)$$

Employing the Kirchhoff hypothesis that the linear filaments of the plate initially perpendicular to the middle surface remain straight and perpendicular to the deformed middle surface and suffer no extensions, \vec{u} and \vec{u}_0 are found to be related as follows:

$$\vec{u} = \vec{u}_0 + z(\vec{n} - \vec{k}), \quad (5)$$

where \vec{n} is a unit normal to the deformed middle surface. Thus, the displacements, and consequently the strains at any point in the plate, can be expressed in terms of the displacements of the middle surface. Strain displacement relations, including nonlinear terms of second degree in the derivatives of displacements, can be found in many texts (see for example [18]). If Equation (5) is substituted into these relations, and it is assumed that all derivatives of tangential displacements u , v , and the squares of derivatives of transverse displacement, w , are of the same order of magnitude and small compared to unity,* then, neglecting terms containing z^2 , the following strain displacement relations are obtained:

*For a physical interpretation of these assumptions see V. V. Novozhilov [18], p. 181.

$$e_{11} = \epsilon_{11} - z\kappa_{11}$$

$$e_{22} = \epsilon_{22} - z\kappa_{22}$$

(6)

$$e_{12} = \epsilon_{12} - z\kappa_{12}$$

$$e_{33} = e_{31} = e_{23} = 0$$

where

$$\epsilon_{11} = u_{,1} + \frac{v}{G_1} G_{1,2} + \frac{1}{2} (w_{,1})^2$$

$$\epsilon_{22} = v_{,2} + \frac{u}{G_2} G_{2,1} + \frac{1}{2} (w_{,2})^2 \quad (7)$$

$$2\epsilon_{12} = v_{,1} + u_{,2} - \frac{v}{G_2} G_{2,1} - \frac{u}{G_1} G_{1,2} + w_{,1}w_{,2}$$

$$\kappa_{11} = w_{,11} + \frac{1}{G_1} G_{1,2} w_{,2}$$

$$\kappa_{22} = w_{,22} + \frac{1}{G_2} G_{2,1} w_{,1} \quad (8)$$

$$2\kappa_{12} = w_{,21} + w_{,12} - \frac{1}{G_2} G_{2,1} w_{,2} - \frac{1}{G_1} G_{1,2} w_{,1}$$

In the above the following notation has been used:

$$(\quad)_{,1} \sim \frac{1}{G_1} \frac{\partial}{\partial \alpha_1} (\quad); \quad (\quad)_{,2} \sim \frac{1}{G_2} \frac{\partial}{\partial \alpha_2} (\quad);$$

$$(\quad)_{,11} \sim \frac{1}{G_1} \frac{\partial}{\partial \alpha_1} (\quad)_{,1}; (\quad)_{,12} \sim \frac{1}{G_2} \frac{\partial}{\partial \alpha_2} (\quad)_{,1}$$

and so on.

The strain components e_{11} and e_{22} are a measure of the change in length of the differential line segments $G_1 d\alpha_1$ and $G_2 d\alpha_2$, respectively. The strain component e_{12} is a measure of the change in the angle between the differential line segments $G_1 d\alpha_1$ and $G_2 d\alpha_2$. Similar physical interpretations can be given to the three other strain components e_{33} , e_{23} , and e_{31} . In view of the assumptions made regarding the magnitude of the derivatives of the middle surface displacements, components of \vec{u} can be written in terms of components of \vec{u}_0 , using Equation (5) as follows:

$$\begin{aligned} u_1 &= u - zw_{,1} \\ u_2 &= v - zw_{,2} \\ u_3 &= w \end{aligned} \tag{9}$$

Stress-Strain Equations

In general, problems in solid mechanics, including thermal effects, are found to be governed by a set of coupled equations describing heat conduction in the solid and mechanical equilibrium of the solid. If the time-gradient of temperature in the solid is large, these equations also contain appropriate inertia terms. Such a general theory, to say the least, is not mathematically simple. However, useful results can be obtained by introducing simplifying assumptions.

If the time-gradient of temperature is small, the corresponding inertia terms can be neglected and if, in addition to this, the coupling terms are also ignored, the resulting theory is called "Uncoupled Quasi-Static Theory." The following formulation is developed according to this theory. Thus two distinct problems are to be solved. The first problem is to obtain the temperature distribution in the solid. It will not be considered here.* The second problem is to obtain the stress distribution in the solid. Here, the temperature distribution appears through the stress-strain equation.

For thin plates it may be assumed that $\sigma_{33} = 0$. This assumption conflicts with the Kirchhoff hypothesis used earlier (see K. Washizu [20], p. 178). However, it is a well-established assumption in thin plate theory, and it will be used here. In view of this assumption the following stress-strain equations for thin plate are obtained:

$$\begin{aligned}\sigma_{11} &= \frac{E}{(1-\nu^2)} (e_{11} + \nu e_{22}) - \frac{Ee^T}{1-\nu}, \\ \sigma_{22} &= \frac{E}{(1-\nu^2)} (e_{22} + \nu e_{11}) - \frac{Ee^T}{1-\nu}, \\ \sigma_{12} &= \frac{E}{1+\nu} e_{12},\end{aligned}\tag{10}$$

where e^T is thermal strain given by

$$e^T = \alpha T(\alpha_1, \alpha_2, z),\tag{11}$$

*Numerous excellent books [19] on this subject are available.

where $T(\alpha_1, \alpha_2, z)$ is temperature distribution in the plate. It is measured from a reference state of uniform temperature. The reference state is also specified to have zero stress and zero strain. Here, α is the coefficient of linear thermal expansion of the plate material.

Equations of Motion

Consider a plate subjected to boundary tractions $F_1(t)$, $F_2(t)$, and $F_3(t)$. Let the region and periphery of the middle surface of the plate be denoted by S and C , respectively (see Figure 3). The direction cosines of the outward normal \vec{v} on C are denoted by ℓ_1 and ℓ_2 ; i.e., $\ell_1 = \cos(\alpha_1, \vec{v})$ and $\ell_2 = \cos(\alpha_2, \vec{v})$. A coordinate, s , is taken along the boundary C such that \vec{v} , s , and z form a right-handed system.

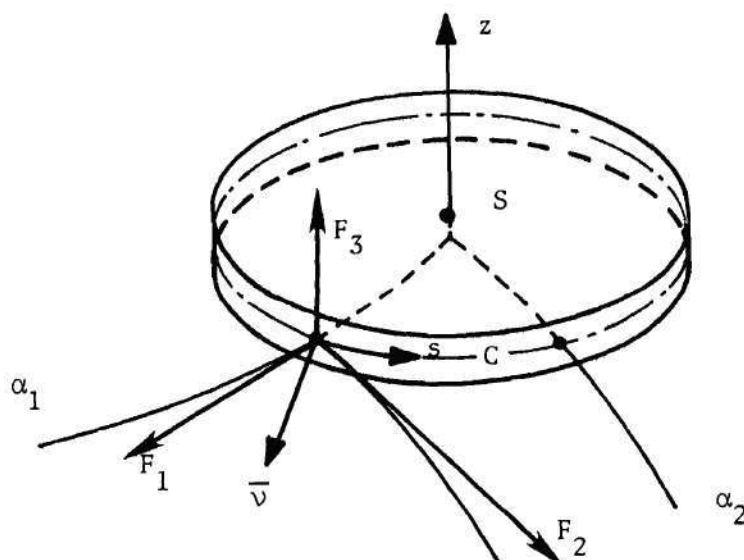


Figure 3. Plate with Boundary Tractions

At a given time, a body in motion can be considered to be in a state of equilibrium if the inertia forces are taken into account (d'Alembert's Principle). Thus, the principle of virtual

work* can be used to obtain the equations of motion. In the development which follows, in-plane inertia forces and rotary inertia effects are neglected. Applying the virtual work principle to the thin plate problem, the following equation must be satisfied at all times:

$$\begin{aligned} \iint_S [\sigma_{11}\delta e_{11} + \sigma_{22}\delta e_{22} + 2\sigma_{12}\delta e_{12} + \rho \frac{\partial^2 u_3}{\partial t^2} \delta u_3] dz dS \\ - \iint_C (F_1\delta u_1 + F_2\delta u_2 + F_3\delta u_3) dz ds = 0, \end{aligned} \quad (12)$$

where ρ is mass density of the plate material, and the δe_{ij} 's and δu_i 's are virtual strains and displacements, respectively. Now, the following operations may be carried out:

- (1) Strains and displacements are substituted in Equation (12) from Equations (6) through (9).
- (2) Integration is carried out with respect to z .
- (3) The divergence theorem is applied to the surface integral.

After performing the above operations, Equation (12) becomes

$$\begin{aligned} -\int_S \left\{ \left[\frac{1}{G_2} (G_2 N_{11})_{,1} + \frac{1}{G_1} (G_1 N_{12})_{,2} + \frac{1}{G_1} N_{12} G_{1,2} - \frac{1}{G_2} N_{22} G_{2,1} \right] \delta u \right. \\ \left. + \left[\frac{1}{G_2} (G_2 N_{12})_{,1} + \frac{1}{G_1} (G_1 N_{22})_{,2} - \frac{1}{G_1} N_{11} G_{1,2} + \frac{1}{G_2} N_{12} G_{2,1} \right] \delta v \right\} dS \end{aligned} \quad (13)$$

*For a statement of principle of virtual work see K. Washizu [20], p. 15.

$$\begin{aligned}
& + \left[\frac{1}{G_2} (G_2 Q_1)_{,1} + \frac{1}{G_1} (G_1 Q_2)_{,2} + \frac{1}{G_2} (G_2 N_{11}^w_{,1} + G_2 N_{12}^w_{,2})_{,1} \right. \\
& \quad \left. + \frac{1}{G_1} (G_1 N_{12}^w_{,1} + G_1 N_{22}^w_{,2})_{,2} - \rho h \frac{\partial^2 w}{\partial t^2} \right] \delta w \Big\} dS \\
& + \int_C \left\{ (\ell_1 N_{11} + \ell_2 N_{12} - \bar{N}_1) \delta u + (\ell_1 N_{12} + \ell_2 N_{22} - \bar{N}_2) \delta v \right. \\
& \quad \left[\ell_1 (N_{11}^w_{,1} + N_{12}^w_{,2} + Q_1) + \ell_2 (N_{12}^w_{,1} + N_{22}^w_{,2} + Q_2) \right. \\
& \quad \left. \left. + \frac{\partial}{\partial s} (M_{vs} - \bar{M}_{vs}) - \bar{Q} \right] \delta w + (\bar{M}_v - M_v) \frac{\partial}{\partial v} \delta w \right\} ds = 0 ,
\end{aligned}$$

where the following definitions for stress resultants and moments have been introduced:*

$$N_{11} = \int \sigma_{11} dz , \quad N_{12} = \int \sigma_{12} dz , \quad N_{22} = \int \sigma_{22} dz , \quad (14)$$

$$M_{11} = \int \sigma_{11} z dz , \quad M_{12} = \int \sigma_{12} z dz , \quad M_{22} = \int \sigma_{22} z dz , \quad (15)$$

$$\bar{N}_1 = \int F_1 dz , \quad \bar{N}_2 = \int F_2 dz , \quad \bar{Q} = \int F_z dz ,$$

$$\bar{M}_1 = \int F_1 z dz , \quad \bar{M}_2 = \int F_2 z dz ;$$

$$\begin{aligned}
Q_1 &= \frac{1}{G_2} [(G_2 M_{11})_{,1} - M_{22} G_{2,1}] + \frac{1}{G_1} [(G_1 M_{12})_{,2} + M_{12} G_{1,2}] ; \\
Q_2 &= \frac{1}{G_1} [(G_1 M_{22})_{,2} - M_{11} G_{1,2}] + \frac{1}{G_2} [(G_2 M_{12})_{,1} + M_{12} G_{2,1}] ;
\end{aligned} \quad (16)$$

*All integrals are taken over the thickness of the plate.

$$M_v = \ell_1^2 M_{11} + 2\ell_1 \ell_2 M_{12} + \ell_2^2 M_{22}, \quad \bar{M}_v = \ell_1 \bar{M}_1 + \ell_2 \bar{M}_2, \quad (17)$$

$$M_{vs} = (M_{22} - M_{11})\ell_1 \ell_2 + M_{12}(\ell_1^2 - \ell_2^2) \text{ and } \bar{M}_{vs} = \ell_1 \bar{M}_2 - \ell_2 \bar{M}_1.$$

Sign convention for the stress resultants and moments are shown in Figure 4. Expressions for the stress resultants and moments in terms of strains are given in Appendix A.

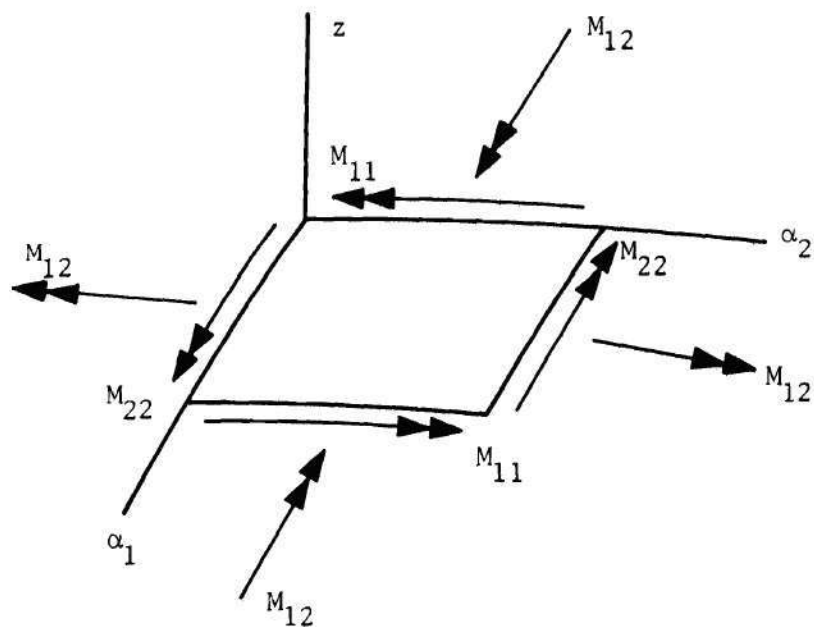
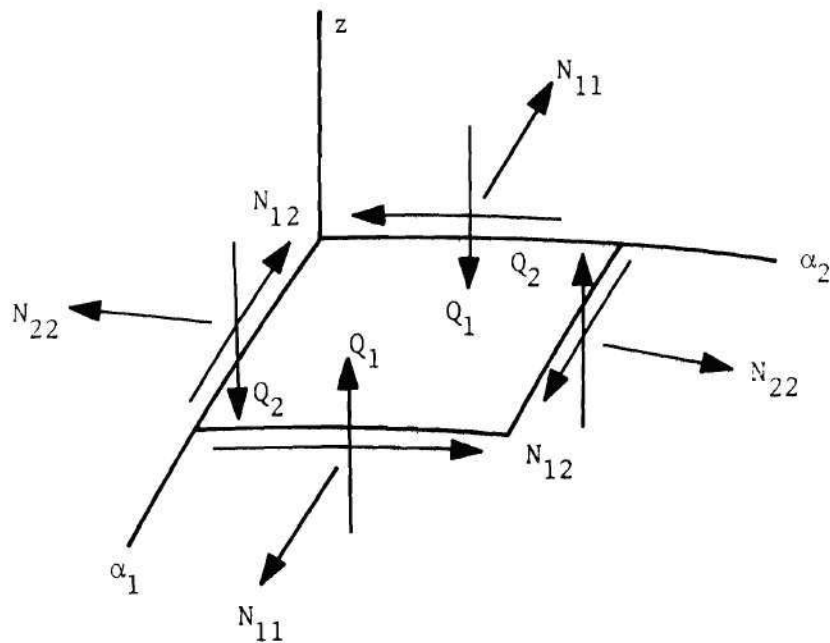
Two states of equilibrium of the plate will be considered. First the "initial state" in which the plate is subjected only to in-plane stresses ($F_3 = 0$) and thermal stresses resulting from a nonuniform temperature distribution. It is also assumed that the external tractions on C and the temperature distribution in S are symmetric with respect to z . The second state is a "perturbed state" of equilibrium in which the initially flat plate can assume a bent configuration.

Initial State of Equilibrium

In the initial state, linearized strain displacement relations are assumed to be valid. Thus, all nonlinear terms in Equation (7) are neglected. All quantities in the initial state are identified with a zero superscript. The use of linearized strain displacement relations and the symmetry of the boundary tractions and temperature distribution yields,

$$u_3^0 = w^0 = 0. \quad (18)$$

In view of Equation (18), Equation (13) becomes



Right-hand Rule

Figure 4. Sign Convention

$$\begin{aligned}
& - \int_S \left\{ \left[\frac{1}{G_2} (G_2 N_{11}^0)_{,1} + \frac{1}{G_1} (G_1 N_{12}^0)_{,2} + \frac{1}{G_1} N_{12}^0 G_{1,2} - \frac{1}{G_2} N_{22}^0 G_{2,1} \right] \delta u^0 \right. \\
& \quad \left. + \left[\frac{1}{G_2} (G_2 N_{12}^0)_{,1} + \frac{1}{G_1} (G_1 N_{22}^0)_{,2} - \frac{1}{G_1} N_{11}^0 G_{1,2} + \frac{1}{G_2} N_{12}^0 G_{2,1} \right] \delta v^0 \right\} ds \\
& + \int_C \left[(\ell_1 N_{11}^0 + \ell_2 N_{12}^0 - N_1^0) \delta u^0 + (\ell_1 N_{12}^0 + \ell_2 N_{22}^0 - \bar{N}_2^0) \delta v^0 \right] ds = 0 .
\end{aligned} \quad (19)$$

For Equation (19) to be valid for arbitrary virtual displacements δu^0 and δv^0 , the following conditions must be satisfied:

In S ,

$$\frac{1}{G_2} (G_2 N_{11}^0)_{,1} + \frac{1}{G_1} (G_1 N_{12}^0)_{,2} + \frac{1}{G_1} N_{12}^0 G_{1,2} - \frac{1}{G_2} N_{22}^0 G_{2,1} = 0 ,$$

and (20)

$$\frac{1}{G_2} (G_2 N_{12}^0)_{,1} + \frac{1}{G_1} (G_1 N_{22}^0)_{,2} - \frac{1}{G_1} N_{11}^0 G_{1,2} + \frac{1}{G_2} N_{12}^0 G_{2,1} = 0 .$$

On C ,

$$\text{either } \ell_1 N_{11}^0 + \ell_2 N_{12}^0 - \bar{N}_1^0 = 0 \text{ or } \delta u^0 = 0 , \quad (21)$$

$$\text{and } \ell_1 N_{12}^0 + \ell_2 N_{22}^0 - \bar{N}_2^0 = 0 \text{ or } \delta v^0 = 0 .$$

Perturbed State of Equilibrium

In this section a state perturbed from the initial state will be considered. The perturbation of the initial state variables will be assumed to be small and they will be identified with a superscript

"*". It is further assumed that the external tractions F_1^0 and F_2^0 , and the temperature distribution do not change ($e^{T*} = 0$). Neglecting higher order terms and noting that Equations (20) and (21) are valid, Equation (13), where virtual displacements are measured from the initial state yields

$$\begin{aligned}
 & - \int_S \left\{ \left[\frac{1}{G_2} (G_2 N_{11}^*),_{,1} + \frac{1}{G_1} (G_1 N_{12}^*),_{,2} + \frac{1}{G_1} N_{12}^* G_{1,2} - \frac{1}{G_2} N_{22}^* G_{2,1} \right] \delta u^* \right. \\
 & + \left[\frac{1}{G_2} (G_2 N_{12}^*),_{,1} + \frac{1}{G_1} (G_1 N_{22}^*),_{,2} - \frac{1}{G_1} N_{11}^* G_{1,2} + \frac{1}{G_2} N_{12}^* G_{2,1} \right] \delta v^* \\
 & + \left[\frac{1}{G_2} (G_2 Q_1),_{,1} + \frac{1}{G_1} (G_1 Q_2),_{,2} + N_{11}^0 (w_{,11} + \frac{1}{G_1} G_{1,2} w_{,2}) \right. \\
 & \quad \left. + N_{22}^0 (w_{,22} + \frac{1}{G_2} G_{2,1} w_{,1}) + 2N_{12}^0 (w_{,12} - \frac{1}{G_2} G_{2,1} w_{,2}) \right. \\
 & \quad \left. - \rho h \frac{\partial^2 w}{\partial t^2} \right] \delta w \Big\} dS \\
 & + \int_C \left\{ (\ell_1 N_{11}^* + \ell_2 N_{12}^*) \delta u^* + (\ell_1 N_{12}^* + \ell_2 N_{22}^*) \delta v^* \right. \\
 & \quad \left. + \left[\ell_1 (N_{11}^0 w_{,1} + N_{12}^0 w_{,2} + Q_1) + \ell_2 (N_{12}^0 w_{,1} + N_{22}^0 w_{,2} + Q_2) + \frac{\partial}{\partial s} M_{vs} \right] \delta w \right. \\
 & \quad \left. - M_v \frac{\partial}{\partial v} \delta w \right\} ds = 0 .
 \end{aligned}$$

For arbitrary δu^* and δv^* , validity of Equation (22) requires that

in S,

$$\frac{1}{G_2} (G_2 N_{11}^*)_{,1} + \frac{1}{G_1} (G_1 N_{12}^*)_{,2} + \frac{1}{G_1} N_{12}^* G_{1,2} - \frac{1}{G_2} N_{22}^* G_{2,1} = 0, \quad (23)$$

$$\frac{1}{G_2} (G_2 N_{12}^*)_{,1} + \frac{1}{G_1} (G_1 N_{22}^*)_{,2} - \frac{1}{G_1} N_{11}^* G_{1,2} + \frac{1}{G_2} N_{12}^* G_{2,1} = 0,$$

and on C

$$\text{either } \ell_1 N_{11}^* + \ell_2 N_{12}^* = 0 \quad \text{or} \quad \delta u^* = 0, \quad (24)$$

$$\text{and } \ell_1 N_{12}^* + \ell_2 N_{22}^* = 0 \quad \text{or} \quad \delta v^* = 0.$$

Solving the differential equation given by Equation (23) subjected to the boundary conditions given by Equation (24), it is found that N_{ij}^* vanish identically. By use of this result and the relations between Q_1 and Q_2 and w (see Appendix A), Equation (22) may be written as,

$$\begin{aligned} & \int_S \left[D \nabla^2 \nabla^2 w - N_{11}^0 (w_{,11} + \frac{1}{G_1} G_{1,2} w_{,2}) \right. \\ & \quad - N_{22}^0 (w_{,22} + \frac{1}{G_2} G_{2,1} w_{,1}) - 2N_{12}^0 (w_{,12} - \frac{1}{G_2} G_{2,1} w_{,2}) \\ & \quad \left. + \rho h \frac{\partial^2 w}{\partial t^2} \right] \delta w \, dS \\ & + \int_C \left\{ \left[\ell_1 (N_{11}^0 w_{,1} + N_{12}^0 w_{,2} + Q_1) + \ell_2 (N_{12}^0 w_{,1} + N_{22}^0 w_{,2} + Q_2) + \frac{\partial}{\partial s} M_{vs} \right] \delta w \right. \\ & \quad \left. - M_v \frac{\partial}{\partial v} \delta w \right\} ds = 0, \end{aligned} \quad (25)$$

where

$$\nabla^2 = \frac{1}{G_1 G_2} \left[\frac{\partial}{\partial \alpha_1} \left(\frac{G_2}{G_1} \frac{\partial}{\partial \alpha_1} \right) + \frac{\partial}{\partial \alpha_2} \left(\frac{G_1}{G_2} \frac{\partial}{\partial \alpha_2} \right) \right]. \quad (26)$$

The expression in brackets under the surface integral sign in Equation (25), if set to zero, is the out-of-plane equation of motion. The expression in brackets under the line integral sign in Equation (25), if set to zero, produces two boundary conditions for bending of thin plates subjected to in-plane stresses. These conditions are not separated into separate equations, but are left in the form of Equation (25) because of the method of solution to be used in the next section.

Parametric Excitation

In this section the transverse motion of the plate in the perturbed state will be considered and a method of studying this motion will be presented. In the next chapter stability of this motion will be considered. Let the initial state of stress in the plate be given by

$$N_{ij}^0(\alpha_1, \alpha_2, t) = \gamma N_{ij}^S(\alpha_1, \alpha_2) + \zeta N_{ij}^T(\alpha_1, \alpha_2) \quad (27)$$

$$+ \beta \psi(t) N_{ij}^D(\alpha_1, \alpha_2), \quad i = 1, 2; \quad j = 1, 2.$$

The symbols β , γ , and ζ are nondimensional factors. N_{ij}^S , N_{ij}^D are the spatial distributions of the stress resultants due to the application of boundary forces \bar{N}_i^{OS} , $\bar{N}_i^{OD} \psi(t)$ ($i = 1, 2$). The spatial distribution of the thermal stress resultants are represented by N_{ij}^T . Here $\psi(t)$ is a periodic function of time.

It may be noted that the N_{ij}^0 appear as coefficients in the differential equation governing the transverse motion. These coefficients may be called parameters. Since the motion arises out of the time dependence of these parameters, the phenomenon is often called parametric excitation.

Method of Solution

One solution approach to this problem is to consider the partial differential equation governing the transverse motion as an initial-boundary value problem. However, the problem is complicated by the spatial and time dependence of N_{ij}^0 . So, instead of proceeding in this manner, an alternative approach, namely, the method of assumed modes will be used.

Let w be represented by a series as*

$$w(\alpha_1, \alpha_2, t) = f_{mn}(t) \phi_{mn}(\alpha_1, \alpha_2) , \quad (28)$$

where $m = 1, 2, \dots$, $n = 1, 2, \dots$, and ϕ_{mn} are assumed modes. The $f_{mn}(t)$ are unknown functions of time. Then a variation of w may be written as

$$\delta w = \frac{\partial w}{\partial f_{pq}} \delta f_{pq} .$$

Substituting for w yields

$$\delta w = \phi_{pq} \delta f_{pq} . \quad (29)$$

*In the rest of this chapter summation convention will be used. According to this convention, a subscript which is repeated in an expression implies summation over the range of that subscript.

Substitution of Equations (27) through (29) into Equation (25) gives a set of equations governing the transverse motion. These equations are

$$a_{pqmn} \frac{d^2}{dt^2} f_{mn} + [b_{pqmn} - \gamma^C_{pqmn} - \beta\psi(t)d_{pqmn} - \zeta e_{pqmn}] f_{mn} = 0, \quad (30)$$

where

$$a_{pqmn} = \int_S \rho h \phi_{mn} \phi_{pq} dS, \quad (31)$$

$$b_{pqmn} = \int_S D(\nabla^2 \nabla^2 \phi_{mn}) \phi_{pq} dS \quad (32)$$

$$+ \int_C \left[(\ell_1 Q_1 + \ell_2 Q_2 + \frac{\partial}{\partial s} M_{vs})_{mn} \phi_{pq} - (M_v)_{mn} \frac{\partial}{\partial v} \phi_{pq} \right] ds,$$

and $p, q, m, n = 1, 2, \dots$. c_{pqmn} , d_{pqmn} , and e_{pqmn} are obtained by substituting N_{ij}^S , N_{ij}^D , and N_{ij}^T , respectively, for N_{ij}^0 ($i = 1, 2$; $j = 1, 2$) in the following expression:

$$\begin{aligned} & \int_S \left[N_{11}^0 (\phi_{mn,11} + \frac{1}{G_1} G_{1,2} \phi_{mn,2}) \right. \\ & \quad + N_{22}^0 (\phi_{mn,22} + \frac{1}{G_2} G_{2,1} \phi_{mn,1}) \\ & \quad \left. + 2N_{12}^0 (\phi_{mn,12} - \frac{1}{G_2} G_{2,1} \phi_{mn,2}) \right] \phi_{pq} dS \\ & + \int_C \left[\ell_1 (N_{11}^0 \phi_{mn,1} + N_{12}^0 \phi_{mn,2}) \right. \\ & \quad \left. + \ell_2 (N_{12}^0 \phi_{mn,1} + N_{22}^0 \phi_{mn,2}) \right] \phi_{pq} ds. \end{aligned} \quad (33)$$

Retaining N terms in the series for w , Equation (30) can be written in matrix form* as

$$\underline{A} \frac{d^2}{dt^2} \underline{\tilde{f}}(t) + [\underline{B} - \gamma \underline{C} - \beta \psi(t) \underline{D} - \zeta \underline{E}] \underline{\tilde{f}}(t) = \underline{0} . \quad (34)$$

The matrices \underline{A} through \underline{E} are square matrices of order N , and they are composed of the elements a_{pqmn} through e_{pqmn} , respectively. The matrices $\underline{\tilde{f}}(t)$ and $\underline{0}$ are column matrices composed of the elements $f_{mn}(t)$ and zeros, respectively.

*A symbol underlined with a " " is a square matrix and, with a "~" is a column matrix.

CHAPTER III

DETERMINATION OF REGIONS OF INSTABILITY

Introduction

In Chapter II the equations of motion in terms of the generalized coordinates $f_{mn}(t)$ were obtained. No attempt will be made to solve these equations in this chapter. The stability of solutions will, however, be discussed. Further, a method for determination of the regions of parameter space in which the solutions are stable or unstable will be presented.

Various portions of the material presented in this chapter may be found in various sources in the literature. However, for the sake of continuity and completeness of presentation, the elements required for the present investigation are given here in some detail.

Form of Solutions

The equations of motion given by Equation (34) can be written as

$$\frac{d^2}{dt^2} \tilde{f}(t) + \underline{\Phi}(t) \tilde{f}(t) = 0, \quad (35)$$

where $\underline{\Phi}(t)$ has the same period, as $\psi(t)$ of Equation (34). Let this period be τ . Introducing the new variables

$$x_j(t) = f_j(t), \quad j = 1, 2, \dots, N$$

$$x_j(t) = \frac{d}{dt} f_{j-N}(t) \quad , \quad j = N+1, N+2, \dots, 2N$$

yields a set of $2N$ equations of first order from Equation (35). These equations are

$$\frac{d}{dt} \underline{x} + \underline{\Xi}(t) \underline{x} = \underline{0} \quad , \quad (36)$$

where \underline{x} consists of the elements x_i ($i = 1, 2, \dots, 2N$) and $\underline{\Xi}(t)$ is a square matrix of order $2N$ given by

$$\underline{\Xi}(t) = \begin{bmatrix} \underline{0} & -\underline{I} \\ \underline{\Phi} & \underline{0} \end{bmatrix} .$$

The symbols $\underline{0}$ and \underline{I} represent a null matrix and an identity matrix, respectively. It is noted here that $\underline{\Xi}(t)$ is periodic with period τ . Thus,

$$\underline{\Xi}(t + \tau) = \underline{\Xi}(t) \quad . \quad (37)$$

Suppose $\underline{X}(t)$ is a fundamental matrix solution* of Equation (36); i.e., it is a square matrix of $2N$ order with each of its columns being a linearly independent solution vector of Equation (36). Hence the matrix $\underline{X}(t)$ is nonsingular for any value of t within the time interval for which Equation (36) is valid. By definition of $\underline{X}(t)$, the following equation holds:

*For a discussion on fundamental matrix solution (also called fundamental system) see Ref. [21].

$$\frac{d}{dt} \underline{X}(t) + \underline{\Xi}(t) \underline{X}(t) = \underline{0} . \quad (38)$$

Let $\underline{X}(t)$ satisfy the initial condition given by

$$\underline{X}(0) = \underline{I} . \quad (39)$$

In view of Equation (37) substitution of $(t + \tau)$ for t in Equation (38) yields

$$\frac{d}{dt} \underline{X}(t + \tau) + \underline{\Xi}(t) \underline{X}(t + \tau) = \underline{0} .$$

Thus $\underline{X}(t + \tau)$ is also a matrix solution of Equation (36) with the initial condition $\underline{X}(\tau)$. This can be represented (the representation satisfies the differential equation and the initial condition) as

$$\underline{X}(t + \tau) = \underline{X}(t) \underline{X}(\tau) . \quad (40)$$

Suppose $\underline{X}(\tau)$ has distinct eigenvalues $\rho_i (i = 1, 2, \dots, 2N)$, then a similarity transformation matrix \underline{Y} can be found* such that

$$\underline{Y}^{-1} \underline{X}(\tau) \underline{Y} = \underline{D} , \quad (41)$$

where \underline{D} is a diagonal matrix with diagonal elements ρ_i . A new matrix solution can then be defined as

$$\underline{Y}(t) = \underline{X}(t) \underline{Y} .$$

*For a proof of this assertion see Ref. [22].

Substituting $(t + \tau)$ for t in this equation, yields using Equation (40)

$$\underline{Y}(t + \tau) = \underline{X}(t) \underline{X}(\tau) \underline{Y} = \underline{X}(t) \underline{Y} \underline{Y}^{-1} \underline{X}(\tau) \underline{Y} ,$$

which becomes by virtue of Equation (41)

$$\underline{Y}(t + \tau) = \underline{Y}(t) \underline{D} .$$

Thus for the i th column \tilde{Y}^i of \underline{Y}

$$\tilde{Y}^i(t + \tau) = \rho_i \tilde{Y}^i(t) . \quad (42)$$

This can be written as*

$$\tilde{Y}^i(t) = \exp\left(\frac{t}{\tau} \ln \rho_i\right) \tilde{X}^i(t) \quad (43)$$

where $\tilde{X}^i(t)$ is a column matrix of periodic functions of time with period τ . The eigenvalues (ρ_i) may be complex, so its natural logarithm can be expressed as

$$\ln \rho_i = \ln |\rho_i| + i \arg \rho_i , \quad 0 < \arg \rho_i < 2\pi . \quad (44)$$

Substituting Equation (44), Equation (43) becomes

$$\tilde{Y}^i(t) = \exp\left(\frac{t}{\tau} \ln |\rho_i|\right) \tilde{X}^i(t) \exp\left(\frac{it}{\tau} \arg \rho_i\right) . \quad (45)$$

*Note that $\exp(\ln \rho_i) = \rho_i$ and by definition $\tilde{X}^i(t + \tau) = \tilde{X}^i(t)$, therefore, substitution of $(t + \tau)$ for t in Equation (43) leads to Equation (42).

Stability of Motion

Stability Condition

A motion governed by Equation (35) and subjected to arbitrary initial conditions can be described by a linear combination of the column vectors \tilde{x}^i of \underline{X} . Therefore if any of the \tilde{x}^i increase without bound with time, the system governed by Equation (35) is unstable. However, \tilde{x}^i 's can be expressed as a linear combination of \tilde{y}^i 's (by definition). Hence, if any of the \tilde{y}^i 's increases without bound with time, at least one of the \tilde{x}^i 's will be unbounded rendering the system unstable.

Whether \tilde{y}^i is bounded or unbounded depends on the absolute value of ρ_i and the following observations can be made from Equation (45):

$$|\rho_i| > 1 \quad ; \quad \text{i.e., } \ln|\rho_i| > 0 \Rightarrow \text{unbounded solution.}$$

$$|\rho_i| < 1 \quad ; \quad \text{i.e., } \ln|\rho_i| < 0 \Rightarrow \text{bounded solution.}$$

$$|\rho_i| = 1 \quad ; \quad \text{i.e., } \ln|\rho_i| = 0 \Rightarrow \text{periodic solution.}$$

Regions of Instability

In the preceding it was found that the stability of the system depends on the absolute values of the eigenvalues ρ_i , which in turn depend on the system parameters (β , γ , ζ , and Θ). It is evident that the parameter space may be divided into regions of stability and instability. In the discussion which follows it is shown that for the problems under consideration, the boundaries of these regions are defined by periodic solutions, (\tilde{y}^i) , with period τ and 2τ . This approach circumvents the often impossible task of determining the

eigenvalues ρ_i , as functions of the system parameters.

For the problems under consideration it can be shown that both of the following statements are true:

- (1) If ρ_i is an eigenvalue, its conjugate is also an eigenvalue (see L. Meirovitch [23], p. 269).
- (2) If ρ_i is an eigenvalue, then $1/\rho_i$ is also an eigenvalue (see Ref. [24]).

The second assertion indicates that if $\rho_i = \pm 1$, then an eigenvalue of multiplicity two occurs. In this case one solution vector \tilde{Y}^i of the form given by Equation (45), and a second one \tilde{Y}^j of the form

$$\tilde{Y}^j(t) = t \exp\left(\frac{t}{\tau} \ln |\rho_i|\right) \tilde{X}^j(t) \exp\left(\frac{it}{\tau} \arg \rho_i\right), \quad (46)$$

can be found (see Ref. [25]). In what follows, it will be assumed that at most one eigenvalue of multiplicity two is present. Therefore, the conjugate of an eigenvalue is also its reciprocal. If this were not true, then associated with any one eigenvalue there would be three more. Namely, its conjugate, its reciprocal, and the conjugate of its reciprocal. All of these would become equal if the eigenvalue became $+1$ or -1 . This permits an eigenvalue of multiplicity four which contradicts the assumption on the multiplicities of eigenvalues. Consider a pair of solutions \tilde{Y}^i and \tilde{Y}^j associated with the eigenvalue ρ_i and its reciprocal $\rho_j = 1/\rho_i$. Then the following cases arise:

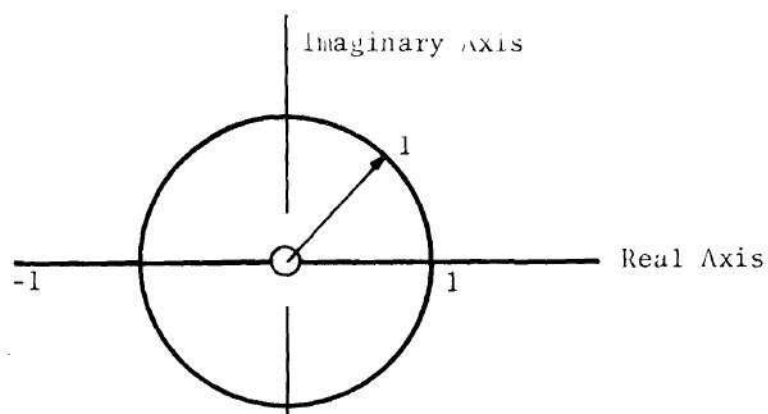
- (1) ρ_i is real and is not equal to ± 1 : here, either $|\rho_i|$ or $|\rho_j|$ is greater than one and the system is unstable.

- (2) ρ_i is real and is equal to +1 or -1: here, $\rho_j = \rho_i$, and \tilde{Y}^i is periodic with period τ or 2τ and \tilde{Y}^j as given by Equation (46) renders the system unstable.
- (3) ρ_i is complex and ρ_j is the conjugate of ρ_i : here, $|\rho_i| = |\rho_j| = 1$ and the system is stable.

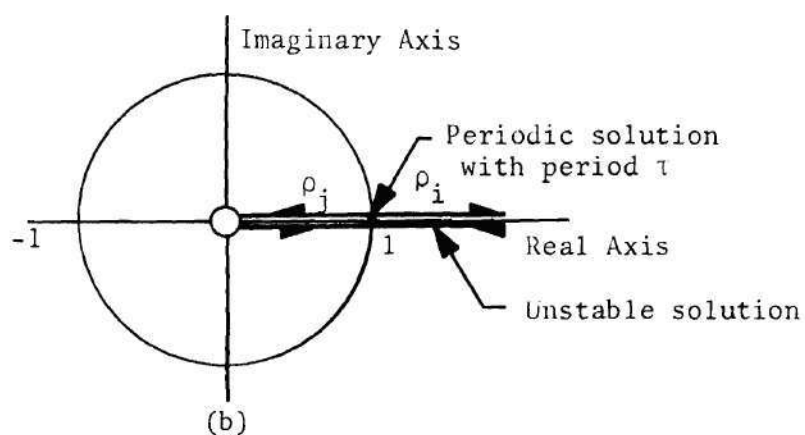
Consider the variation of a pair of eigenvalues ρ_i and ρ_j in the complex plane (Figure 5). ρ_j is the reciprocal and also the conjugate of ρ_i . If the system parameters are varied, ρ_i and ρ_j may move along two paths depicted by heavy lines in Figure (5a). Since ρ_i and ρ_j are reciprocal of each other, they must both be either real or complex. Also ρ_i and ρ_j , being eigenvalues of a nonsingular matrix, cannot be equal to zero. Consider a point in parameter space where ρ_i is equal to +1. At this point, a periodic solution of period τ exists. If the system parameters are now continuously changed, the two eigenvalues may change along two paths. Along one both the eigenvalues are real and along the other they are complex.

Along the first path, shown by a heavy line in Figure (5b), $|\rho_i| > 1$ as it moves to the right, and the system is unstable. As the system parameters are changed, ρ_j at first decreases. However, ρ_j cannot become zero. Therefore, somewhere between zero and one ρ_j starts to increase and eventually becomes unity. The system again permits a periodic solution of period τ . Thus two solutions with period τ bound a region of instability.

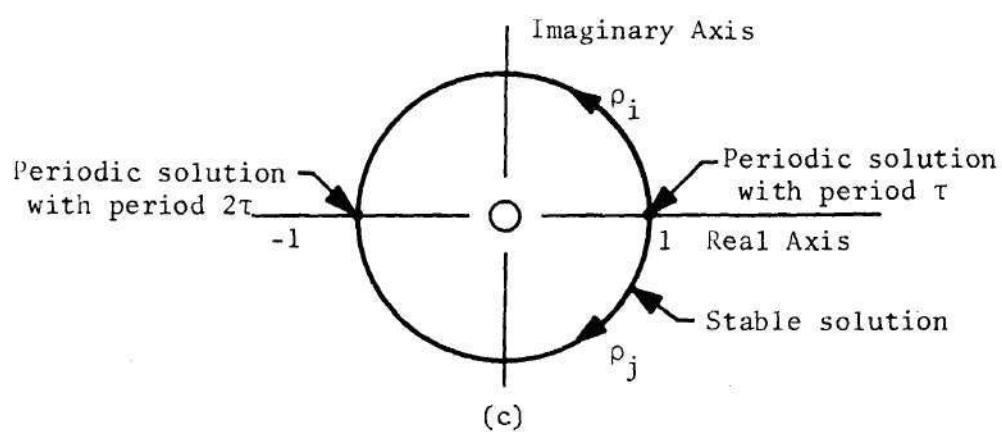
On the second path, shown by a heavy line in Figure (5c), $|\rho_i| = |\rho_j| = 1$, and the system is stable. As the system parameters are changed, both the eigenvalues ultimately become equal to -1 and



(a)



(b)



(c)

Figure 5. Variation of Eigenvalues in Complex Plane

the system has a solution of period 2τ . Therefore two solutions of period τ and 2τ form the boundaries of the stable region.

The above observations can also be made by starting from a point where $\rho_i = -1$. Therefore it follows that two solutions of the same period (τ or 2τ) bound an unstable region and two solutions of different periods bound a stable region. However, on the boundaries ($\rho_i = \rho_j = +1$) multiple eigenvalues occur. Consequently, the system has an unbounded solution and is unstable.

Determination of the Boundaries

Criteria for the existence of solutions with period τ and 2τ of Equation (34) will be developed here. These criteria may be used to obtain the boundaries of the regions of stability and instability. In the problems to be investigated $\psi(t)$ is given by $\cos\theta t$. Substituting for $\psi(t)$, Equation (34) can be rewritten as

$$\underline{F} \frac{d^2}{dt^2} \underline{\tilde{f}}(t) + [\underline{I} - \gamma \underline{G} - \zeta \underline{E} - \beta \underline{B} \cos\theta t] \underline{\tilde{f}}(t) = \underline{0} \quad (48)$$

where,

$$\underline{F} = \underline{B}^{-1} \underline{A} \quad , \quad \underline{G} = \underline{B}^{-1} \underline{C}$$

$$\underline{E} = \underline{B}^{-1} \underline{E} \quad , \quad \underline{B} = \underline{B}^{-1} \underline{D} \quad .$$

Solutions of Equation (48) with period τ and 2τ can be represented by Fourier series of the form

$$\underline{\tilde{f}}(t) = \frac{1}{2} \underline{\xi}_0 + \sum_{\eta=2,4,6}^{\infty} (\underline{\phi}_{\eta} \sin \frac{\eta\theta t}{2} + \underline{\xi}_{\eta} \cos \frac{\eta\theta t}{2}) \quad (49)$$

and

$$\tilde{f}(t) = \frac{1}{2} \underline{\xi}_0 + \sum_{\eta=1,2,3}^{\infty} (\underline{\phi}_{\eta} \sin \frac{\eta \theta t}{2} + \underline{\xi}_{\eta} \cos \frac{\eta \theta t}{2}) . \quad (50)$$

In Equations (49) and (50) $\underline{\xi}_0$, $\underline{\xi}_{\eta}$, and $\underline{\phi}_{\eta}$ are column vectors consisting of Fourier coefficients. Substituting, in turn, Equations (49) and (50) into Equation (48), and requiring in each case that not all the coefficient vectors vanish simultaneously yields the following existence conditions (see Appendix B for details) for solutions with period 2τ ,

$$\begin{vmatrix} \underline{I} - \underline{\gamma G} - \underline{\zeta E} + \frac{\beta}{2} \underline{B} - \frac{\theta^2}{4} \underline{F} & -\frac{\beta}{2} \underline{B} & \underline{0} \\ -\frac{\beta}{2} \underline{B} & \underline{I} - \underline{\gamma G} - \underline{\zeta E} - \frac{9}{4} \theta^2 \underline{F} & -\frac{\beta}{2} \underline{B} \\ \underline{0} & -\frac{\beta}{2} \underline{B} & \underline{I} - \underline{\gamma G} - \underline{\zeta E} - \frac{25}{4} \theta^2 \underline{F} \\ . & . & . \end{vmatrix} = 0 . \quad (51)$$

For solutions with period τ ,

$$\begin{vmatrix} \underline{I} - \underline{\gamma G} - \underline{\zeta E} - \theta^2 \underline{F} & -\frac{\beta}{2} \underline{B} & \underline{0} \\ -\frac{\beta}{2} \underline{B} & \underline{I} - \underline{\gamma G} - \underline{\zeta E} - 4\theta^2 \underline{F} & -\frac{\beta}{2} \underline{B} \\ \underline{0} & -\frac{\beta}{2} \underline{B} & \underline{I} - \underline{\gamma G} - \underline{\zeta E} - 9\theta^2 \underline{F} \\ . & . & . \end{vmatrix} = 0 , \quad (52)$$

and

$$\begin{vmatrix}
 I - \gamma \underline{G} - \zeta \underline{E} & -\beta \underline{B} & \underline{0} \\
 -\frac{\beta}{2} \underline{B} & I - \gamma \underline{G} - \zeta \underline{E} - \theta^2 \underline{F} & -\frac{\beta}{2} \underline{B} \\
 0 & -\frac{\beta}{2} \underline{B} & I - \gamma \underline{G} - \zeta \underline{E} - 4\theta^2 \underline{F} \\
 \cdot & \cdot & \cdot
 \end{vmatrix} = 0. \quad (53)$$

All the determinants appearing in Equations (51) through (53) are infinite determinants and they are convergent.* It may be noted that the elements of these determinants are square matrices of order N (see Equation (34)).

Using Equations (51) through (53) the boundaries can be determined. Evaluation of infinite determinants can be approximated by considering the associated principal minor determinants of increasing order. The desired accuracy in determination of the boundaries can thus be achieved.

Principal Instability Regions

Some insight into the locations of the regions of instability in the parameter space can be gained by considering some limiting cases. Let γ, ζ be zero and β be very small ($\beta \rightarrow 0$), then Equations (51) through (53) reduce to the form

$$\left| I - \frac{n^2 \theta^2}{4} \underline{F} \right| = 0, \quad n = 1, 2, 3, \dots \quad (54)$$

*For details see Ref. [5], p. 218.

If $1/\omega_i^2$ ($i = 1, 2, \dots, N$) are the eigenvalues of the matrix \underline{F} , then roots of Equation (54) are given by

$$\Theta^* = \frac{2\omega_i}{\eta}, \quad (55)$$

$$i = 1, 2, \dots, N \quad ; \quad \eta = 1, 2, 3, \dots$$

It is possible to visualize that as the parameters assume nonzero values, a region of instability develops corresponding to each Θ^* . The regions of instability emanating from the Θ^* 's for which $\eta = 1$ ($\Theta^* = 2\omega_i$) are called the "principal regions" of instability. Some study of Equation (48) reveals that ω_i are the natural frequencies of the plate associated with assumed modes in Equation (28).

CHAPTER IV

EQUATIONS OF MOTION FOR A CIRCULAR AND A RECTANGULAR PLATE

Introduction

In this chapter the results developed in Chapter II are applied to rectangular and circular plate problems. For each case the appropriate equations will be established for problems involving thermal stresses and parametric excitation. Dynamic stability analysis will be carried out in Chapter V.

In the presentation which follows, attention is directed to the procedures used to compute the coefficients of Equation (30) which governs the transverse motion of the plates. For convenient reference Equation (30) of Chapter II is given below:

$$a_{pqmn} \frac{d^2}{dt^2} f_{mn}(t) + [b_{pqmn} - \gamma c_{pqmn} - \beta \psi(t) d_{pqmn} - \zeta e_{pqmn}] f_{mn}(t) = 0. \quad (30)$$

Circular Plate

Definition of the Problem

A polar coordinate system for problems involving a circular region is appropriate, and it will be employed throughout this section. In polar coordinates α_1 and α_2 will be denoted by r and θ respectively, and G_1 and G_2 are given by

$$G_1 = 1 \quad , \quad G_2 = r \quad . \quad (56)$$

Consider a circular plate (see Figure 6), of radius b , clamped on its boundary and subjected to boundary forces given by

$$\bar{N}_1^0 = -\bar{N}_r^S - \bar{N}_r^D \cos \theta t$$

(57)

and

$$\bar{N}_2^0 = 0 \quad ,$$

where \bar{N}_r^S and \bar{N}_r^D are the amplitudes of the static and dynamic components of the boundary force, respectively. Further, let the plate contain a concentric hot spot of radius, a , and uniform temperature \bar{T} . The faces of the plate are insulated and the boundary is maintained at zero temperature. Using results from theory of heat conduction (Ref. [19]), the temperature distribution in the plate, for $a \leq r \leq b$, is found to be governed by the differential equation

$$r \frac{d^2 T}{dr^2} + \frac{dT}{dr} = 0 \quad , \quad (58)$$

with boundary conditions

$$T(a) = \bar{T} \quad \text{and} \quad T(b) = 0 \quad . \quad (59)$$

Solving the differential equation (58) subjected to the boundary conditions given by Equation (59), and noting that the hot spot is maintained at temperature \bar{T} , the temperature distribution in the plate is found to be,

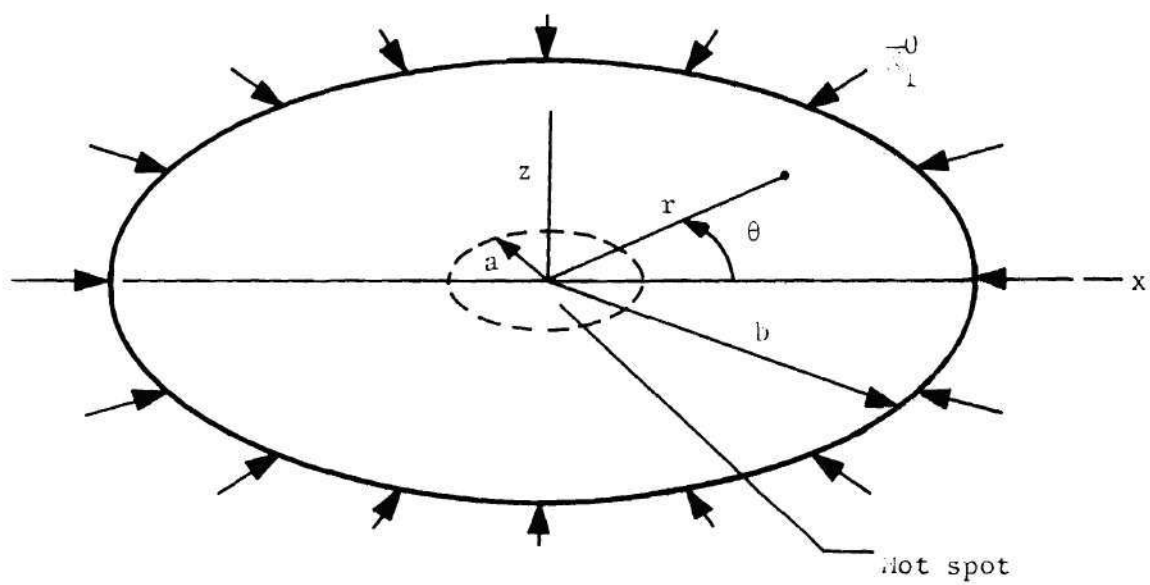


Figure 6. Circular Plate with Boundary Forces and a Hot Spot

$$T = \bar{T} \quad , \quad 0 \leq r \leq a \quad , \quad (60)$$

$$T = \bar{T} \ln \left(\frac{b}{r} \right) / \ln \left(\frac{b}{a} \right) \quad , \quad a \leq r \leq b \quad .$$

Initial State of Equilibrium

The stress resultants in the initial state satisfy Equation (20) which in polar coordinate take the following forms:

$$\begin{aligned} \frac{1}{r} \frac{\partial}{\partial r} (r N_{rr}^0) + \frac{1}{r} \frac{\partial}{\partial \theta} N_{r\theta}^0 - \frac{1}{r} N_{\theta\theta}^0 &= 0 \quad . \\ \frac{1}{r} \frac{\partial}{\partial r} (r N_{r\theta}^0) + \frac{1}{r} \frac{\partial}{\partial \theta} N_{\theta\theta}^0 + \frac{1}{r} N_{r\theta}^0 &= 0 \quad . \end{aligned} \quad (61)$$

The direction cosines of the outward normal to the plate boundary are

$$\lambda_1 = 1 \quad \text{and} \quad \lambda_2 = 0 \quad . \quad (62)$$

In view of Equation (62), the boundary conditions given by Equation (21) become

$$N_{rr}^0 \Big|_{r=b} = \bar{N}_1^0$$

(63)

and

$$N_{r\theta}^0 \Big|_{r=b} = \bar{N}_2^0 \quad ,$$

where \bar{N}_1^0 and \bar{N}_2^0 are given by Equation (57).

The stress resultants for the initial state can be found by solving Equation (61) in conjunction with Equation (A1) of Appendix A and the linearized form of strain displacement relations given by Equation (7). The required boundary conditions are given by Equation

(63). The stress resultants, thus found, can be written in the form of Equation (27) as

$$\begin{aligned}
 N_{rr}^0 &= \gamma N_{rr}^S + \zeta N_{rr}^T + \beta \cos \Theta t N_{rr}^D \\
 N_{\theta\theta}^0 &= \gamma N_{\theta\theta}^S + \zeta N_{\theta\theta}^T + \beta \cos \Theta t N_{\theta\theta}^D \\
 N_{r\theta}^0 &= \gamma N_{r\theta}^S + \zeta N_{r\theta}^T + \beta \cos \Theta t N_{r\theta}^D
 \end{aligned} \tag{64}$$

where

$$\gamma = \frac{\bar{N}_r^S}{D} b^2, \quad \beta = \frac{\bar{N}_r^D}{D} b^2, \quad \zeta = \frac{E \alpha \bar{T} h b^2}{D} \tag{65}$$

$$N_{rr}^D = N_{\theta\theta}^D = N_{rr}^S = N_{\theta\theta}^S = -\frac{D}{b^2}, \quad N_{r\theta}^D = N_{r\theta}^S = 0 \tag{66}$$

$$N_{rr}^T = \begin{cases} -N_0^T, & 0 \leq r \leq a \\ -N_0^T - \frac{D}{4b^2 \ln(b/a)} \left[1 - \frac{a^2}{r^2} + 2 \ln\left(\frac{a}{r}\right) \right], & a < r < b \end{cases} \tag{67}$$

$$N_{\theta\theta}^T = \begin{cases} -N_0^T, & 0 \leq r \leq a \\ N_{rr}^T - \frac{D}{2b^2 \ln(b/a)} \left(\frac{a^2}{r^2} - 1 \right), & a < r < b \end{cases} \tag{68}$$

$$N_{r\theta}^T = 0 \tag{69}$$

and

$$N_0^T = \frac{D}{4b^2 \ln(b/a)} \left[\frac{a^2}{b^2} + 2 \ln \left(\frac{b}{a} \right) - 1 \right] . \quad (70)$$

E. W. Parkes [26] solved the thermal stress problem for a circular plate with a concentric hot spot. Some results from his article have been used to obtain Equations (66) through (69).

Equations of Parametric Excitation

In Chapter II the equation governing parametric excitation was reduced to Equation (30). In this section the coefficients of Equation (30) are found for the circular plate problem. To this end, it is necessary to state the form of ϕ_{mn} 's to be used in the deflection function of Equation (28). Let the ϕ_{mn} 's be the eigenfunctions of free transverse vibration of a clamped circular plate of radius b . Therefore ϕ_{mn} is given by (see Ref. [27]),

$$\phi_{mn}(r, \theta) = [J_m(\lambda_{mn} \frac{r}{b}) - T_{mn} I_m(\lambda_{mn} \frac{r}{b})] \cos m\theta , \quad (71)$$

$$m = 0, 1, 2, \dots ; \quad n = 1, 2, 3, \dots ,$$

where J_m and I_m are ordinary and modified Bessel functions of first kind of order m , respectively, and λ_{mn} is the n th root of the characteristic equation

$$J_{m+1}(\lambda_{mn}) + T_{mn} I_{m+1}(\lambda_{mn}) = 0 . \quad (72)$$

The symbol T_{mn} represents the ratio

$$T_{mn} = \frac{J_m(\lambda_{mn})}{I_m(\lambda_{mn})} .$$

The λ_{mn} 's are related to the natural frequencies (ω_{mn}) of free transverse vibration by the equation

$$\lambda_{mn}^4 = \frac{1}{D} \omega_{mn}^2 \rho h b^4 \quad (73)$$

It is important to note that the eigenfunctions satisfy the following orthogonality relations (see Ref. [27]):

$$\int_0^b \int_0^{2\pi} \rho h \phi_{mn}(r, \theta) \phi_{pq}(r, \theta) r d\theta dr = 0, \quad m \neq p \text{ or } n \neq q, \quad (74)$$

$$\int_0^b \int_0^{2\pi} D \phi_{mn}(r, \theta) \nabla^2 \nabla^2 \phi_{pq}(r, \theta) r d\theta dr = 0, \quad m \neq p \text{ or } n \neq q, \quad (75)$$

where ∇^2 is given by Equation (26) which in polar coordinates is

$$\nabla^2 = \frac{1}{r} \frac{\partial}{\partial r} \left(r \frac{\partial}{\partial r} \right) + \frac{1}{r^2} \frac{\partial^2}{\partial \theta^2}. \quad (76)$$

It should also be noted that the eigenfunctions satisfy the following boundary conditions on the boundary of the plate:

$$\left. \frac{\partial}{\partial \nu} \phi_{mn}(r, \theta) \right|_{r=b} = 0, \quad (77)$$

$$\left. \phi_{mn}(r, \theta) \right|_{r=b} = 0.$$

Having defined the functions ϕ_{mn} , it is now possible to determine the coefficients a_{pqmn} through e_{pqmn} of Equation (30). In view of Equation (77), it is clear that line integrals in Equations (31) and (32) and in Expression (33) vanish. They then take the

following form in polar coordinates:

$$a_{pqmn} = \int_0^b \int_0^{2\pi} \rho h \phi_{mn}(r, \theta) \phi_{pq}(r, \theta) r d\theta dr, \quad (78)$$

$$b_{pqmn} = \int_0^b \int_0^{2\pi} D \phi_{pq}(r, \theta) \nabla^2 \nabla^2 \phi_{mn}(r, \theta) r d\theta dr, \quad (79)$$

and

$$\begin{aligned} \int_0^b \int_0^{2\pi} \left[N_{rr}^0 \frac{\partial^2}{\partial r^2} \phi_{mn}(r, \theta) + N_{\theta\theta}^0 \left(\frac{1}{r} \frac{\partial}{\partial r} + \frac{1}{r^2} \frac{\partial^2}{\partial \theta^2} \right) \phi_{mn}(r, \theta) \right. \\ \left. + 2 N_{r\theta}^0 \left(\frac{1}{r} \frac{\partial^2}{\partial r \partial \theta} - \frac{1}{r^2} \frac{\partial}{\partial \theta} \right) \phi_{mn}(r, \theta) \right] \phi_{pq}(r, \theta) r d\theta dr. \end{aligned} \quad (80)$$

Substitution of the static, dynamic and thermal stress resultant distributions from Equations (65) through (69) into Expression (80) yields results for c_{pqmn} , d_{pqmn} , and e_{pqmn} , respectively. Since $N_{r\theta}^0$ is zero (see Equations (66), (69), and (64)), the expression (80) can be rewritten as

$$\int_0^b \int_0^{2\pi} \left[N_{rr}^0 \frac{\partial^2}{\partial r^2} \phi_{mn}(r, \theta) + N_{\theta\theta}^0 \left(\frac{1}{r} \frac{\partial}{\partial r} + \frac{1}{r^2} \frac{\partial^2}{\partial \theta^2} \right) \phi_{mn}(r, \theta) \right] \phi_{pq}(r, \theta) r d\theta dr. \quad (81)$$

Substitution of ϕ_{mn} and ϕ_{pq} from Equation (71) into Equation (78) and use of Equation (74) yields, after carrying out necessary

integration* for $m = p$ and $n = q$,

$$a_{pqmn} = \begin{cases} 0 & , \quad m \neq p \text{ or } n \neq q \\ \epsilon \pi \rho h b^2 J_m^2(\lambda_{mn}) & , \quad m = p \text{ and } n = q , \end{cases} \quad (82)$$

where the symbol ϵ has the following values:

$$\epsilon = \begin{cases} 2 & , \quad m = 0 , \\ 1 & , \quad m \neq 0 . \end{cases} \quad (83)$$

To evaluate b_{pqmn} it is first observed that ϕ_{mn} , being an eigenfunction of the corresponding free transverse vibration problem, satisfies the differential equation

$$\nabla^2 \nabla^2 \phi_{mn} = \frac{\lambda_{mn}^4}{b^4} \phi_{mn} . \quad (84)$$

Use of this result in Equation (79) leads to

$$b_{pqmn} = \frac{D \lambda_{mn}^4}{b^4} \int_0^b \int_0^{2\pi} \phi_{mn}(r, \theta) \phi_{pq}(r, \theta) r d\theta dr . \quad (85)$$

Again using the procedure used to determine a_{pqmn} , Equation (85) may be written

$$b_{pqmn} = \begin{cases} 0 & , \quad m \neq p \text{ or } n \neq q \\ \epsilon \pi \frac{D \lambda_{mn}^4}{b^2} J_m^2(\lambda_{mn}) & , \quad m = p \text{ and } n = q . \end{cases} \quad (86)$$

*For a technique of evaluating the resulting integral see W. P. Reid [28].

Evaluation of c_{pqmn} and d_{pqmn} involves integration of Expression (81) after substituting the indicated stress resultant distributions. It is seen from Equation (66) that the static and dynamic stress resultant distributions are identical,* therefore, it can be concluded that

$$d_{pqmn} = c_{pqmn} . \quad (87)$$

Substituting N_{rr}^S and $N_{\theta\theta}^S$ for N_{rr}^0 and $N_{\theta\theta}^0$ from Equation (66) in Expression (81) leads to

$$c_{pqmn} = - \frac{D}{b^2} \int_0^b \int_0^{2\pi} \phi_{pq}(r, \theta) \nabla^2 \phi_{mn}(r, \theta) r d\theta dr . \quad (88)$$

Substitution of ϕ_{mn} and ϕ_{pq} from Equation (71) into Equation (88) yields, after carrying out necessary integrations,

$$\frac{c_{pqmn}}{\epsilon \pi} = \begin{cases} 0 , & m \neq p \\ \frac{4D\lambda_{mq}^2 \lambda_{mn}^2}{b^2 (\lambda_{mn}^4 - \lambda_{mq}^4)} [\lambda_{mn} J_m(\lambda_{mq}) J_{m+1}(\lambda_{mn}) \\ - \lambda_{mq} J_m(\lambda_{mn}) J_{m+1}(\lambda_{mq})] , & m = p \text{ and } n \neq q \\ \frac{D}{b^2} T_{mn}^2 \lambda_{mn} [\lambda_{mn} I_{m+1}^2(\lambda_{mn}) + 2m I_m(\lambda_{mn}) I_{m+1}(\lambda_{mn})] , & m = p \text{ and } n = q . \end{cases} \quad (89)$$

*As noted earlier, in-plane inertia effects are neglected in the development used here.

Some integration formulae are needed to arrive at Equation (89).

These are given in Appendix C.

The coefficients e_{pqmn} are determined by substituting the thermal stress resultant distribution from Equations (67) and (68) into Equation (81). After some rearranging, the result is

$$\begin{aligned}
 -\frac{4b^2}{D} e_{pqmn} = & \frac{4b^2}{D} N_0^T \int_0^b \int_0^{2\pi} \phi_{pq}(r, \theta) \nabla^2 \phi_{mn}(r, \theta) r d\theta dr \\
 & + \frac{1}{\ln(b/a)} \int_a^b \int_0^{2\pi} \left\{ \left[1 - \left(\frac{a}{r}\right)^2 + 2 \ln \left(\frac{a}{r}\right) \right] \nabla^2 \phi_{mn}(r, \theta) \right. \\
 & \left. + 2 \left[\left(\frac{a}{r}\right)^2 - 1 \right] \left(\frac{1}{r} \frac{\partial}{\partial r} + \frac{1}{r^2} \frac{\partial^2}{\partial \theta^2} \right) \phi_{mn}(r, \theta) \right\} \phi_{pq}(r, \theta) r d\theta dr .
 \end{aligned} \tag{90}$$

The integrations involved in Equation (90) can be carried out analytically for the variable θ . It can be found that

$$e_{pqmn} = 0 \quad , \quad m \neq p . \tag{91}$$

Analytical integration with respect to the variable r can be done only for the first integral in Equation (90). The second integral is to be evaluated numerically. The result of the first integral is given in Appendix C.

Rectangular Plate

Definition of the Problem

A rectangular plate with a cartesian coordinate system is shown in Figure 7. In cartesian coordinates α_1 and α_2 will be denoted by x

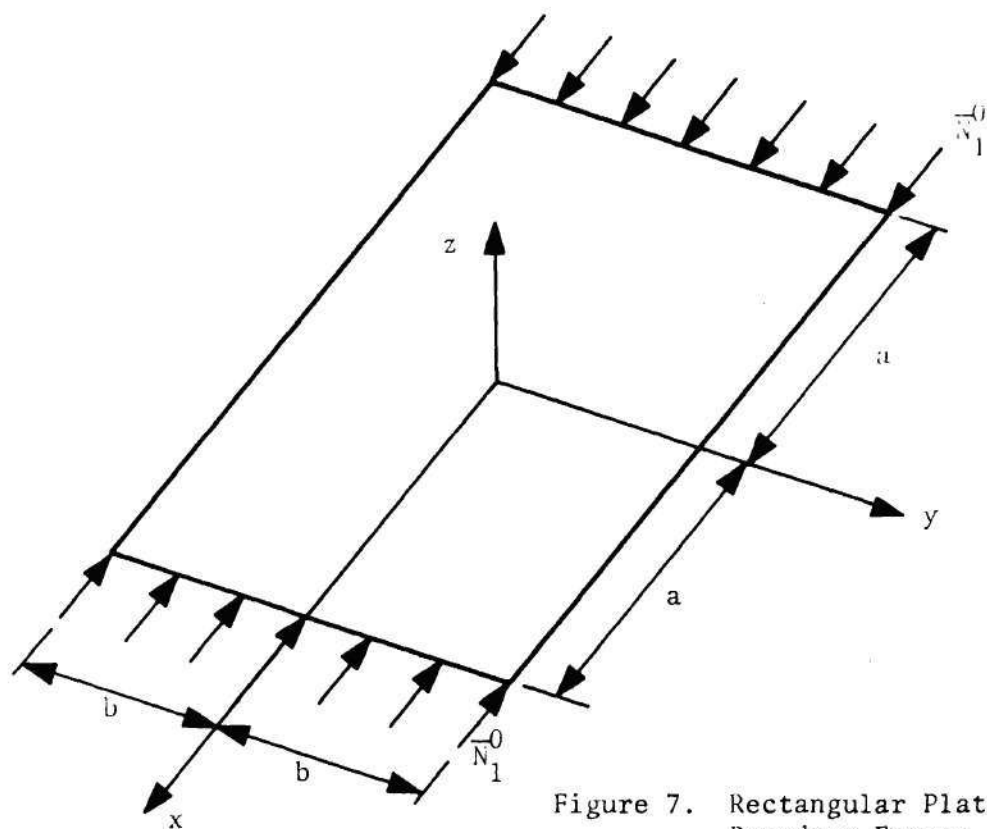


Figure 7. Rectangular Plate with Boundary Forces

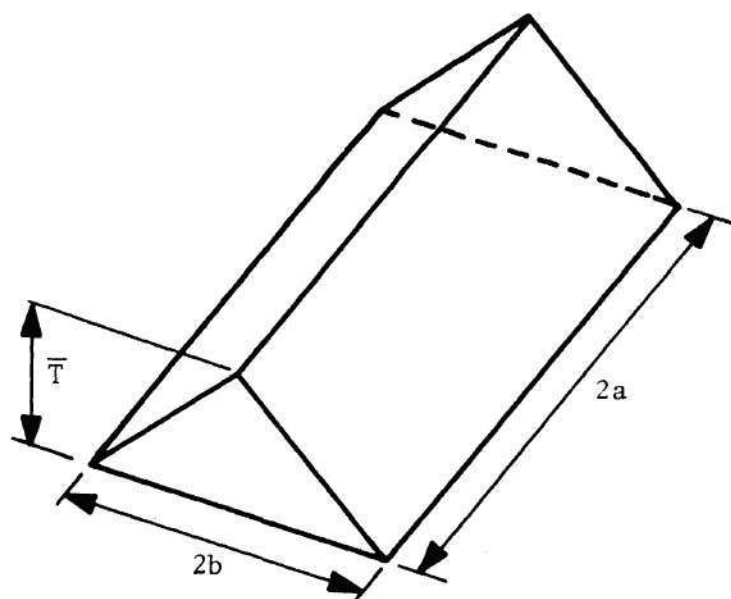


Figure 8. Tent-Like Temperature Distribution

and y respectively, and G_1 and G_2 are given by

$$G_1 = G_2 = 1 . \quad (92)$$

Let the plate be simply supported on its boundary and, subjected to boundary forces

$$\bar{N}_1^0 = \begin{cases} +(\bar{N}_x^S + \bar{N}_x^D \cos \theta t) & , \text{ on } x = \pm a \\ 0 & , \text{ on } y = \pm b \end{cases} \quad (93)$$

and

$$\bar{N}_2^0 = 0 ,$$

where \bar{N}_x^S and \bar{N}_x^D are the amplitudes of the static and dynamic components of the boundary force, respectively. Further, let the plate be subjected to a tent-like temperature distribution (see Figure 8) with maximum temperature \bar{T} .

Initial State of Equilibrium

The stress resultants in the initial state satisfy Equation (20). In cartesian coordinates these equations take the following forms:

$$\begin{aligned} \frac{\partial}{\partial x} N_{xx}^0 + \frac{\partial}{\partial y} N_{xy}^0 &= 0 . \\ \frac{\partial}{\partial x} N_{xy}^0 + \frac{\partial}{\partial y} N_{yy}^0 &= 0 . \end{aligned} \quad (94)$$

The direction cosines of the outward normal to the plate boundary are

$$\begin{aligned}
 x = \pm a : \quad \ell_1 &= \pm 1, \quad \ell_2 = 0. \\
 y = \pm b : \quad \ell_1 &= 0, \quad \ell_2 = \pm 1.
 \end{aligned}
 \tag{95}$$

In view of Equation (95), the boundary conditions given by Equation (21) become

on $x = \pm a$;

$$\begin{aligned}
 N_{11}^0 &= \pm \bar{N}_1^0, \\
 N_{12}^0 &= \pm \bar{N}_2^0,
 \end{aligned}
 \tag{96}$$

on $y = \pm b$;

$$\begin{aligned}
 N_{12}^0 &= \pm \bar{N}_1^0, \\
 N_{22}^0 &= \pm \bar{N}_2^0,
 \end{aligned}
 \tag{97}$$

where \bar{N}_1^0 and \bar{N}_2^0 are given by Equation (93). The stress resultants in the plate for this state may be found by solving Equation (94), in conjunction with Equation (A1) of Appendix A, and the linearized form of strain displacement relations given by Equation (7). The required boundary conditions are given by Equations (96) and (97). The stress resultants will be found in two parts and superposed to obtain the required result. In the first part, the stress resultants are determined, as outlined above, for the plate at uniform temperature subjected to boundary forces given by Equation (93). The second part consists of finding the thermal stress resultants for the plate

subjected to the tent-like temperature distribution, with zero boundary forces. This thermal stress problem has been solved by R. R. Heldenfels and W. M. Roberts [29], using Kantorovich's method, and their results will be used here. This is an approximate method in which a boundary value problem involving a partial differential equation is converted to a boundary value problem involving an ordinary differential equation.*

The stress resultants obtained by proceeding as above can be written in the form of Equation (27), as

$$\begin{aligned} N_{xx}^0 &= \gamma N_{xx}^S + \zeta N_{xx}^T + \beta \cos \theta t N_{xx}^D \\ N_{yy}^0 &= \gamma N_{yy}^S + \zeta N_{yy}^T + \beta \cos \theta t N_{yy}^D \\ N_{xy}^0 &= \gamma N_{xy}^S + \zeta N_{xy}^T + \beta \cos \theta t N_{xy}^D \end{aligned} \quad (99)$$

where

$$\gamma = \frac{\bar{N}_x^S}{D} b^2, \quad \beta = \frac{\bar{N}_x^D}{D} b^2, \quad \zeta = \frac{E \alpha \bar{T} h b^2}{D} \quad (100)$$

$$\begin{aligned} N_{xx}^D &= N_{xx}^S = -\frac{D}{b^2} \\ N_{yy}^D &= N_{yy}^S = N_{xy}^S = N_{xy}^D = 0 \end{aligned} \quad (101)$$

$$\begin{aligned} N_{xx}^T &= \frac{D}{2b^2} \left(2 \frac{y}{b} - 1 \right) \left(1 + B_1 \sinh R_1 \frac{x}{a} \sin R_2 \frac{x}{a} \right. \\ &\quad \left. + B_2 \cosh R_1 \frac{x}{a} \cos R_2 \frac{x}{a} \right) \end{aligned} \quad (102)$$

*For details see Ref. [30].

$$N_{yy}^T = \frac{D}{12b^2} \left(1 - 3 \frac{y^2}{b^2} + 2 \frac{y^3}{b^3} \right) (D_1 \sinh R_1 \frac{x}{a} \sin R_2 \frac{x}{a} \quad (103)$$

$$+ D_2 \cosh R_1 \frac{x}{a} \cos R_2 \frac{x}{a})$$

$$N_{xy}^T = \frac{D}{2b^2} \left(\frac{y}{b} - \frac{y^2}{b^2} \right) (D_3 \sinh R_1 \frac{x}{a} \cos R_2 \frac{x}{a} \quad (104)$$

$$+ D_4 \cosh R_1 \frac{x}{a} \sin R_2 \frac{x}{a})$$

The symbols B_1 , B_2 , R_1 , R_2 , and D_1 through D_4 represent constants which are defined in Appendix D. The equations (102) through (103) are valid for the region $0 \leq y \leq b$. The corresponding stress resultant distributions in the rest of the plate are identical to those in this region.

Equations of Parametric Excitation

In order to determine the coefficients of the governing equation (Equation (30)) of parametric excitation, it is necessary to define the functions ϕ_{mn} to be used in Equation (28). Let the ϕ_{mn} 's be the symmetric eigenfunctions of free transverse vibration of the simply supported rectangular plate. Therefore ϕ_{mn} is given by (Ref. [27])

$$\phi_{mn}(x,y) = \cos \frac{m\pi x}{2a} \cos \frac{n\pi y}{2b}, \quad (105)$$

$$m = 1, 3, 5, \dots; n = 1, 3, 5, \dots$$

These eigenfunctions satisfy the following orthogonality relations:

$$\int_{-b}^b \int_{-a}^a \rho h \phi_{mn}(x,y) \phi_{pq}(x,y) dx dy = 0, \quad m \neq p \text{ or } n \neq q, \quad (106)$$

$$\int_{-b}^b \int_{-a}^a D \phi_{mn}(x,y) \nabla^2 \nabla^2 \phi_{pq}(x,y) dx dy = 0, \quad m \neq p \text{ or } n \neq q, \quad (107)$$

where ∇^2 is given by Equation (26), which in cartesian coordinate is

$$\nabla^2 = \frac{\partial^2}{\partial x^2} + \frac{\partial^2}{\partial y^2}. \quad (108)$$

It should also be noted that the eigenfunctions satisfy the following boundary conditions on the boundary of the plate:

$$\begin{aligned} \phi_{mn}(x,y) \Big|_C &= 0, \\ (M_v)_{mn} \Big|_C &= 0, \end{aligned} \quad (109)$$

where C is the boundary of the middle surface of the plate. M_v is defined by Equation (17) and is expressible in terms of $w(x,y)$ (see Appendix A) and, consequently, in terms of ϕ_{mn} 's (see Equation (28)). The term in the resulting expression for M_v corresponding to ϕ_{mn} is $(M_v)_{mn}$.

In view of Equation (109) it is clear that line integrals in Equations (31) and (32) and in Expression (33) vanish. These then take the following form in cartesian coordinates:

$$a_{pqmn} = \int_{-b}^b \int_{-a}^a \rho h \phi_{mn}(x,y) \phi_{pq}(x,y) dx dy, \quad (110)$$

$$b_{pqmn} = \int_{-b}^b \int_{-a}^a D \phi_{pq}(x,y) \nabla^2 \nabla^2 \phi_{mn}(x,y) dx dy, \quad (111)$$

and

$$\int_{-b}^b \int_{-a}^a [N_{xx}^0 \frac{\partial^2}{\partial x^2} \phi_{mn}(x,y) + N_{yy}^0 \frac{\partial^2}{\partial y^2} \phi_{mn}(x,y) + 2 N_{xy}^0 \frac{\partial^2}{\partial x \partial y} \phi_{mn}(x,y)] \phi_{pq}(x,y) dx dy . \quad (112)$$

The coefficients a_{pqmn} through e_{pqmn} are determined in the same way as used previously for the circular plate in this chapter. The results follow:

For $m \neq p$ or $n \neq q$,

$$a_{pqmn} = b_{pqmn} = c_{pqmn} = 0 . \quad (113)$$

For $m = p$ and $n = q$,

$$\begin{aligned} a_{pqmn} &= \rho h a b , \\ b_{pqmn} &= \rho h a b \omega_{mn}^2 , \end{aligned} \quad (114)$$

$$c_{pqmn} = \frac{m^2 \pi^2}{4} \frac{D}{ab} ,$$

$$d_{pqmn} = c_{pqmn} . \quad (115)$$

In contrast to the circular plate problem, in this case the integrations involved in the evaluation of e_{pqmn} can be carried out analytically and the resulting expression is given in Appendix D. The coefficients e_{pqmn} had earlier been evaluated in Ref. [14]. They were reevaluated by the author and some expressions in Ref. [14] were found to contain typographical errors.

CHAPTER V

PRESENTATION AND DISCUSSION OF RESULTS

Introduction

In the preceding chapter the equations of motion for a circular and a rectangular plate were obtained. These equations may be re-written in the form of Equation (48). Using Equations (51) through (53), the boundaries of the regions of instability may be determined in each case. In the last section of Chapter III it was observed that each of these regions can be associated with a value of excitation frequency, namely, Θ^* given by Equation (55). Thus, there are an infinite number of such regions.

Theoretically the motion of the plate becomes unbounded when the system parameters (β , γ , ζ , and Θ) take values within a region of instability or on its boundaries. In reality, however, the presence of "damping"* and the development of the nonlinear effect of middle surface stretching due to bending attenuates the motion. Thus, though motion with large amplitude can develop, it is bounded. The resulting motions for all the regions of instability are not equally severe. In fact, experimental investigation (see Ref. [6]) of some plate problems show that the motion in the principal region of instability is by far the most severe. In the subsequent sections the results for the first

*In contrast to ordinary vibration, a linear analysis of parametric excitation with linear viscous damping shows that unbounded motion is possible. For details see Ref. [5].

principal region (i.e., the one corresponding to the lowest natural frequency for each of the plate problems) are presented. The thermal effect on these regions is discussed. In addition the thermal and thermal-static combination buckling problems are considered.

This study is primarily concerned with the effect of thermal stresses on the principal regions. The effect of static mean stress has been already considered in other investigations (see Chapter I). Thus, in what follows the parameter characterizing static mean stress, namely γ , will be set equal to zero. Consequently, Equation (48) becomes

$$\underline{F} \frac{d^2}{dt^2} \underline{f}(t) + [\underline{I} - \underline{\zeta} \underline{E} - \underline{\beta} \underline{B} \cos \theta t] \underline{f}(t) = \underline{0} , \quad (116)$$

where, as was previously defined,

$$\underline{F} = \underline{B}^{-1} \underline{A} , \quad \underline{E} = \underline{B}^{-1} \underline{E} \quad \text{and} \quad \underline{B} = \underline{B}^{-1} \underline{D} \quad (117)$$

For this case the Equation (51) for the boundaries become

$$\begin{vmatrix} \underline{I} - \underline{\zeta} \underline{E} + \frac{\underline{\beta}}{2} \underline{B} - \frac{\theta^2}{4} \underline{F} & - \frac{\underline{\beta}}{2} \underline{B} & \underline{0} \\ - \frac{\underline{\beta}}{2} \underline{B} & \underline{I} - \underline{\zeta} \underline{E} - \frac{9}{4} \theta^2 \underline{F} & - \frac{\underline{\beta}}{2} \underline{B} \\ \underline{0} & - \frac{\underline{\beta}}{2} \underline{B} & \underline{I} - \underline{\zeta} \underline{E} - \frac{25}{4} \theta^2 \underline{F} \end{vmatrix} = 0 . \quad (118)$$

In order to present the results in a general form, two new parameters associated with β and ζ are defined as

$$\bar{\beta} = \frac{\beta}{\beta_{cr}} \quad \text{and} \quad \bar{\zeta} = \frac{\zeta}{\zeta_{cr}}, \quad (119)$$

where β_{cr} is the critical value of β associated with static buckling of the plate subjected to the stress distribution characterized by β . The symbol ζ_{cr} represents the critical value of the temperature parameter for the thermal buckling of the plate. β_{cr} values for both the problems considered here are readily available in the literature [31]. The values of ζ_{cr} have to be determined.

The ranges of parameters $\bar{\beta}$ and $\bar{\zeta}$ are to be selected in such a way that simultaneous application of thermal stresses and the stresses due to oscillating load do not give rise to buckling. In the linearized theory used, buckling represents a limiting response. Such buckling is hereafter referred to as combination buckling. It is most likely to occur when $\cos\theta t$ becomes unity; i.e., when the oscillating load is a maximum.

Computational Procedure

The Matrices

Formulae for the elements of the matrices A, B, D, and E are given in Chapter IV for both the circular and rectangular plate problems. In both cases the coefficients depend on the ratio a/b which for the circular plate is the ratio of hot spot radius to plate radius. For the rectangular plate it is the ratio of length to breadth of the plate. For a given value of a/b the matrix elements can be calculated using the formulae given, and the corresponding matrices can then be formed. The matrices appearing in Equation (116)

are obtained by using Equation (117).

Thermal Buckling

The governing equation for the thermal buckling problem is obtained by setting β equal to zero and requiring that \tilde{f} be time-independent. Equation (116) then becomes

$$[\underline{I} - \zeta \underline{E}] \tilde{f} = \underline{0} . \quad (120)$$

For the existence of nontrivial solutions of Equation (120) the following must be satisfied:

$$|[\underline{I} - \zeta \underline{E}]| = 0 . \quad (121)$$

It is evident that the critical temperature parameters are eigenvalues of the eigenvalue problem described by Equation (120). The smallest eigenvalue, (ζ_{cr}) , was found by a matrix iteration technique [32]. Iteration was continued until convergence to seven significant digits was achieved.

Combination Buckling

The governing equation for the combination buckling problem is obtained from Equation (116) by requiring \tilde{f} be time-independent and by setting $\cos \theta t$ equal to unity. The equation thus obtained is

$$[\underline{I} - \beta \underline{B} - \zeta \underline{E}] \tilde{f} = \underline{0} . \quad (122)$$

Equation (122) may be rewritten as

$$[\underline{E}^{-1} [\underline{I} - \beta \underline{B}] - \zeta \underline{I}] \tilde{f} = \underline{0} . \quad (123)$$

Requiring that the solutions of Equation (123) be nontrivial leads to

the following buckling criterion:

$$| [E^{-1} [I - \beta B] - \zeta I] | = 0 . \quad (124)$$

By taking different values of β , and using a matrix iteration technique, the lowest value of ζ satisfying Equation (124) was found. Iteration was continued until convergence to seven significant digits was achieved.

Principal Region of Instability

Boundaries of the principal regions of instability are obtained from Equation (118). Usually the values of the parameters β and ζ are fixed. Then, solving for the frequency parameter, Θ , for which the determinant in Equation (118) becomes zero yields a point on the boundary of a region of instability. These values of the excitation frequency are called the boundary frequencies. Taking both signs (positive and negative) in Equation (118) gives the frequency values for the two boundaries of each region.

Since the determinant in Equation (118) is an infinite determinant, the calculations can best be performed by systematically considering the first, second, and higher order principal minor determinants. This is equivalent to retaining the first three, four, and more terms in the Fourier expansion of Equation (50) for periodic solutions of period 2τ . The difference between two successive approximations serves as a practical estimate of the accuracy of the calculation. The order of principal minor used will be called the order of approximation.

The accuracy of the boundaries also depends on the spatial

approximating functions used and the number of terms retained in the series expansion of w in Equation (28). These functions model the mass and stiffness properties of the plate. The approximating functions used in this study are the eigenfunctions of free transverse vibration. Therefore, they accurately represent the mass properties of the corresponding modes. A set of these functions which yield satisfactory convergence for the combination buckling problem can also be expected to model the stiffness properties satisfactorily. This basis is used here to select the set of functions for the calculation of the boundary frequencies.

The boundary frequencies were determined from the approximating finite determinants by a scanning technique. For given values of ζ and β the approximating determinants were evaluated by changing θ^2 in steps. The value of θ^2 for which the determinant became zero or two successive values of θ^2 for which the determinant changed sign were noted.

Presentation of Results

Circular Plate

Thermal Buckling. The thermal stress distributions in the plate which are given by Equations (67) through (69) are axisymmetric with a compressive radial stress. Axisymmetric buckling of the plate is considered here. Therefore, the use of axisymmetric eigenfunctions ($m = 0$ in Equation (71)) is approximate.

ζ_{cr} was determined for nine values (0.1 through 0.9) of hot spot radius, and the results are shown in Figure 9. Use of the first four axisymmetric eigenfunctions resulted in satisfactory convergence.

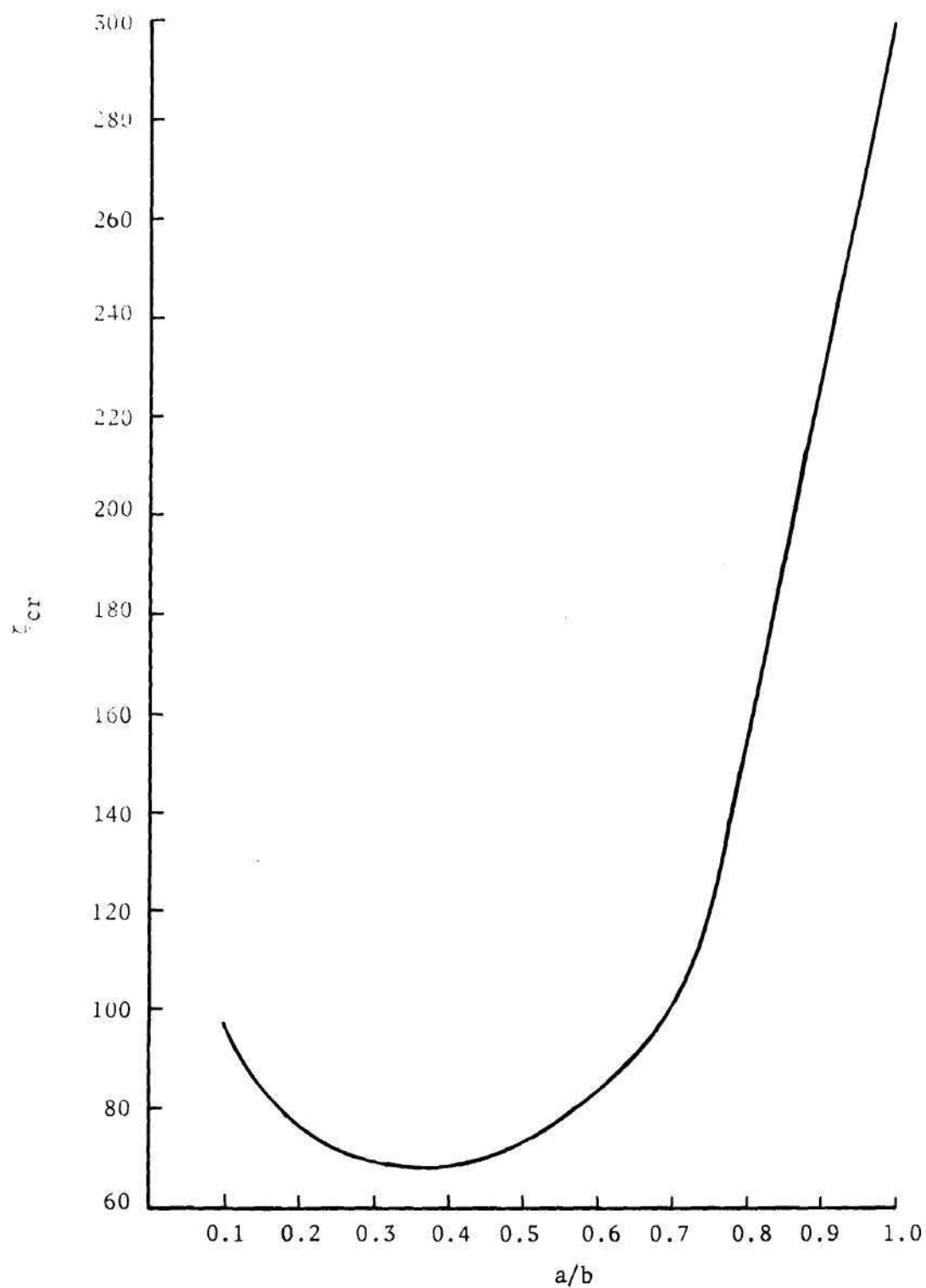


Figure 9. Critical Temperature Parameter vs. Hot Spot Radius

Table 1 gives the values of ζ_{cr} obtained by retaining various terms in the deflection function for hot spot radius 0.1b.

Table 1. Values of ζ_{cr} for $a = 0.1b$ Using $\phi_{on}(r, \theta)$

Values of n	ζ_{cr}
1,2	98.058
1,2,3	97.223
1,2,3,4	97.122

Combination Buckling. In this case again axisymmetric eigenfunctions were used. The calculations were carried out for one value of hot spot radius $a = 0.1b$. The results for the first principal region for this case are presented in the next section. For nine values of $\bar{\beta}$ (0.1 through 0.9) the lowest value of $\bar{\zeta}$ that would cause buckling was determined. These values of $\bar{\beta}$ and $\bar{\zeta}$ are plotted in Figure 10.

Use of the first four eigenfunctions resulted in satisfactory convergence. Table 2 gives the values of $\bar{\zeta}$ for $\bar{\beta} = 0.5$ obtained by retaining various terms in the deflection function.

Table 2. Values of $\bar{\zeta}$ for $\bar{\beta} = 0.5$ Using $\phi_{on}(r, \theta)$

Values of n	$\bar{\zeta}$
1,2	0.52661
1,2,3	0.52588
1,2,3,4	0.52559

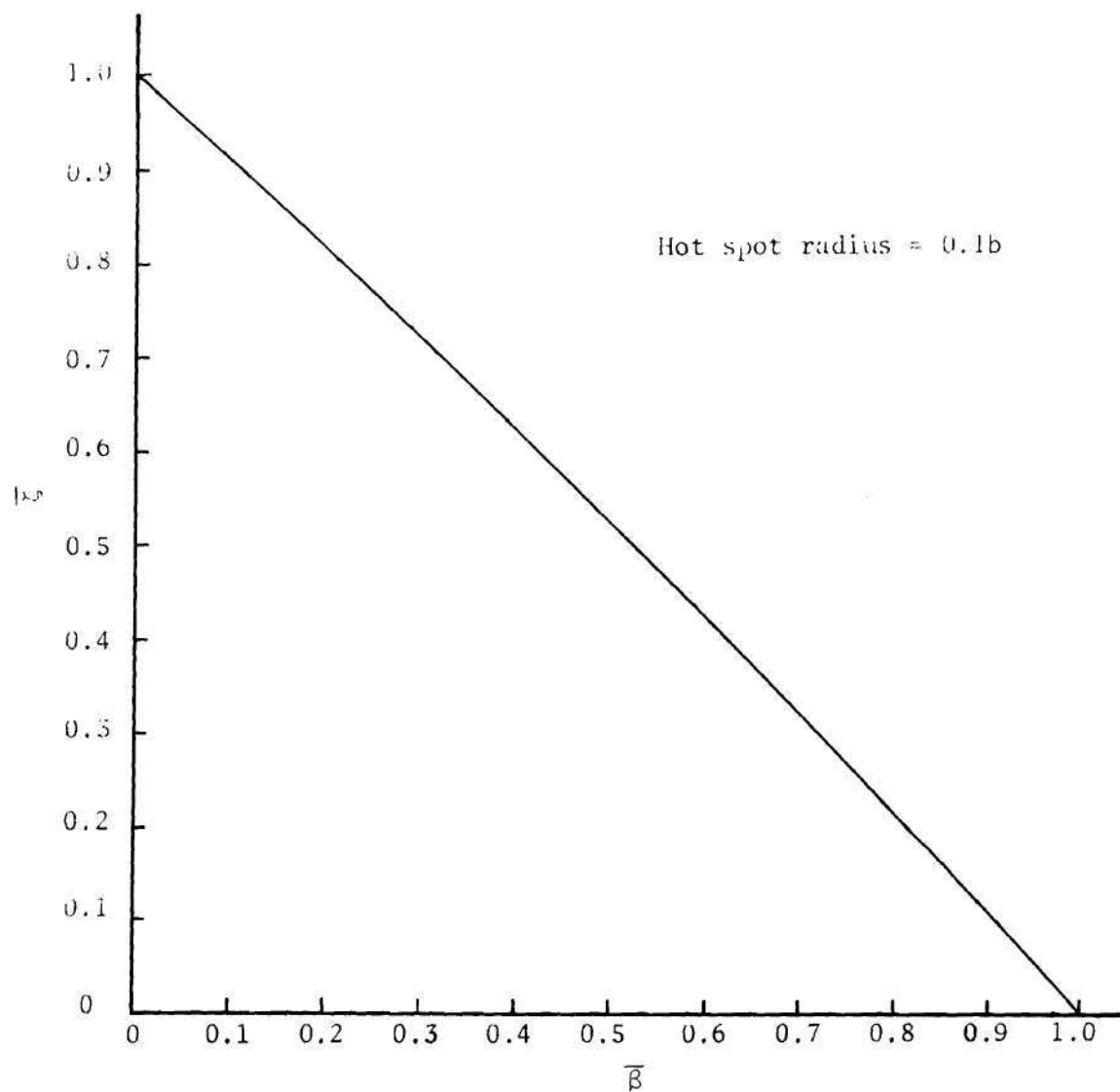


Figure 10. Combination Buckling of Circular Plate

Principal Region of Instability. Results presented here are for a hot spot radius a equal to $0.1b$. The boundary frequencies for the first principal region were found. A step size of $(\theta/\omega_{01})^2 = 0.005$, where ω_{01} is the smallest natural frequency of transverse vibration, was used. A range of six values $(0, 0.1, 0.2, 0.3, 0.4, 0.5)$ for both of the parameters $\bar{\zeta}$ and $\bar{\beta}$ was considered.

The first four axisymmetric eigenfunctions were used in the deflection function. Thus, the matrices appearing in the determinant of Equation (118) were of fourth order. First and second order approximations of the infinite determinant were used to obtain the boundary frequencies. Boundary frequencies for these two approximations were almost identical for small values of $\bar{\beta}$ and $\bar{\zeta}$. For higher values small differences were found. The boundary frequencies obtained from first and second order approximations for upper and lower boundaries are presented in Tables 3 and 4, respectively, for three values of $\bar{\beta}$ and $\bar{\zeta}$. The two entries in each position represent the second and first order approximations, respectively.

The boundaries of the first principal region are plotted in Figure 11 as plots of excitation frequency ratio (θ/ω_{01}) vs. $\bar{\beta}$ and in Figure 12 as plots of θ/ω_{01} vs. $\bar{\zeta}$. The plotted points represent the computed values from the second order approximation.

Rectangular Plate

Thermal Buckling. The thermal buckling problem for the rectangular plate was investigated in Ref. [14]. However, a critical temperature parameter (ζ_{cr}) was not tabulated for various aspect ratios of the plate. In the study presented here the boundaries of the first principal

Table 3. Circular Plate--Upper Boundary Frequency $(\theta/\omega_{01})^2$

$\bar{\beta} \backslash \bar{\zeta}$	0.3	0.4	0.5
0.3	3.660, 3.660	3.335, 3.330	2.995, 2.990
0.4	3.865, 3.860	3.540, 3.530	3.200, 3.190
0.5	4.065, 4.060	3.745, 3.730	3.410, 3.390

Table 4. Circular Plate--Lower Boundary Frequency $(\theta/\omega_{01})^2$

$\bar{\beta} \backslash \bar{\zeta}$	0.3	0.4	0.5
0.3	2.470, 2.460	2.125, 2.110	1.770, 1.750
0.4	2.280, 2.250	1.940, 1.900	1.585, 1.540
0.5	2.100, 2.050	1.760, 1.690	1.415, 1.330

region for a plate of aspect ratio unity were determined. ζ_{cr} for aspect ratio unity was also computed.

Satisfactory convergence was achieved by retaining four terms in the series of w . Table 5 shows the convergence of the critical temperature parameter as more terms are taken in the deflection function.

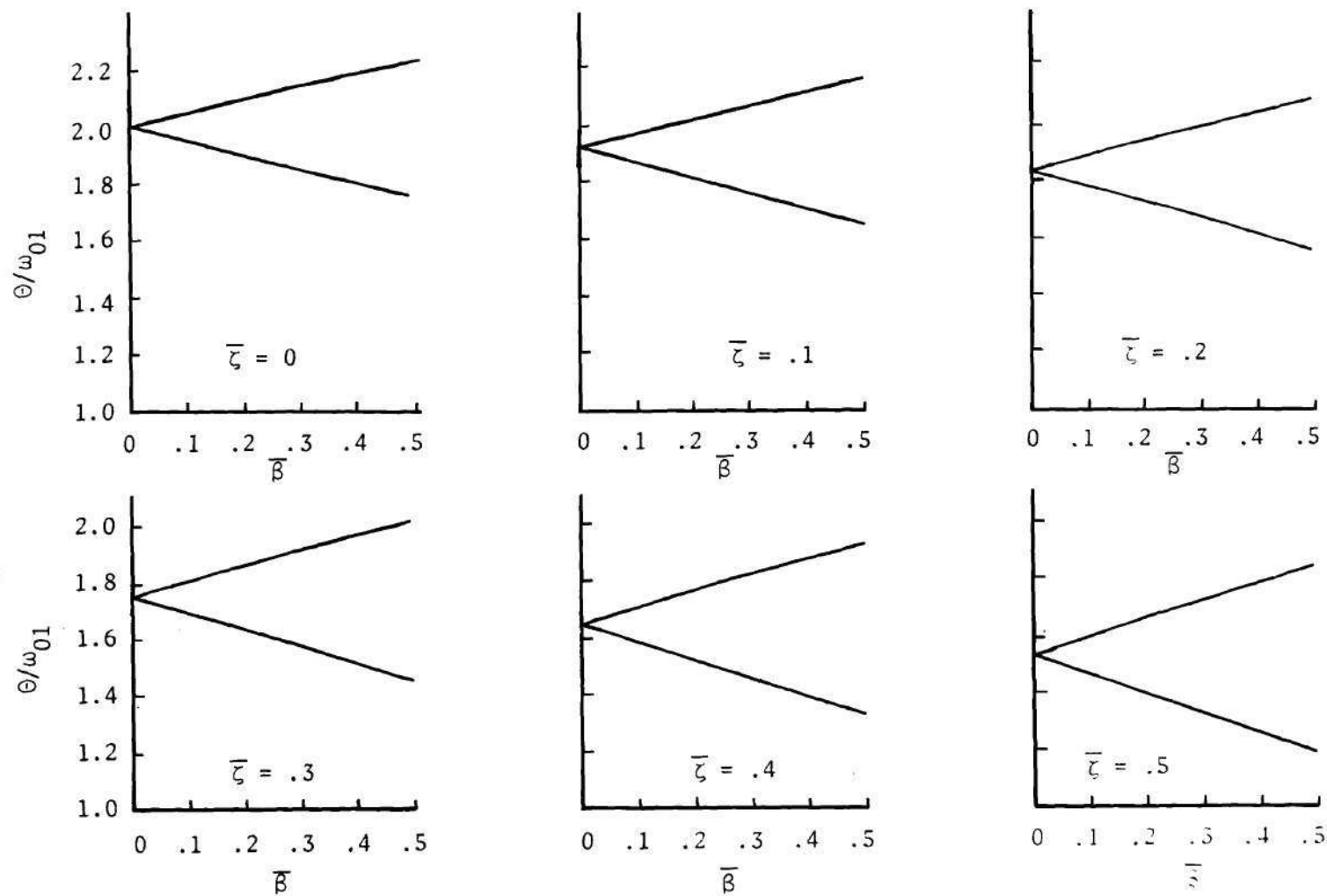


Figure 11. First Principal Region of Instability of the Circular Plate. Excitation Frequency vs. Oscillating Load

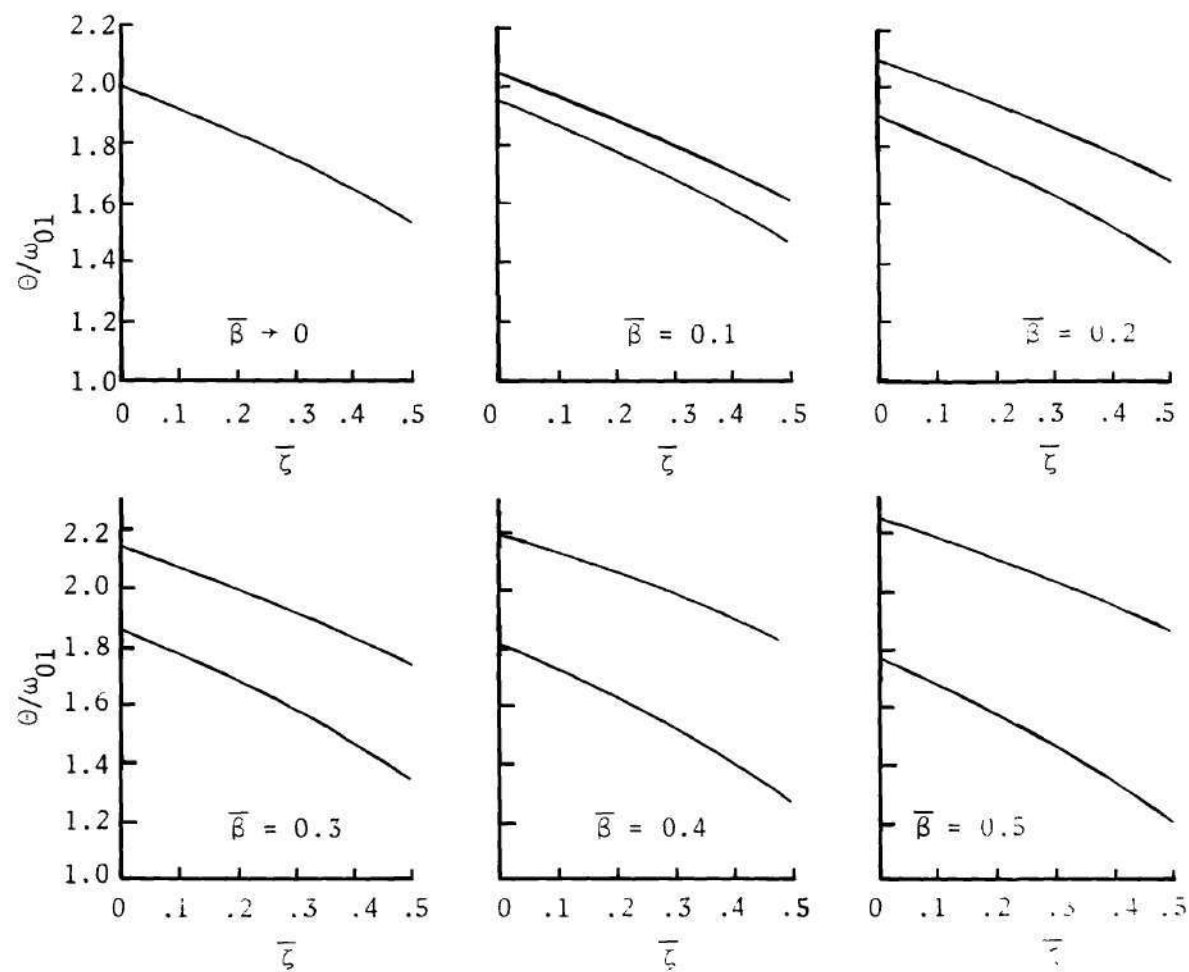


Figure 12. First Principal Region of Instability of the Circular Plate.
Excitation Frequency vs. Temperature Parameter

Table 5. Values of ζ_{cr} for $a/b = 1$

Terms retained	ζ_{cr}
ϕ_{11}, ϕ_{31}	87.823
$\phi_{11}, \phi_{13}, \phi_{31}$	80.314
$\phi_{11}, \phi_{13}, \phi_{31}, \phi_{33}$	80.240

Combination Buckling. The calculations were carried out for an aspect ratio unity. For nine values of $\bar{\beta}$ (0.1 through 0.9) the lowest value of $\bar{\zeta}$ that would cause buckling was determined. These values of $\bar{\beta}$ and $\bar{\zeta}$ are plotted in Figure 13. Use of four terms in the series of w resulted in satisfactory convergence. The convergence of the values of $\bar{\zeta}$ for a typical case ($\beta = 0.5$) obtained by including various terms in the deflection function is shown in Table 6.

Table 6. Values of $\bar{\zeta}$ for $\bar{\beta} = 0.5$

Terms retained	$\bar{\zeta}$
ϕ_{11}, ϕ_{31}	0.56229
$\phi_{11}, \phi_{13}, \phi_{31}$	0.53762
$\phi_{11}, \phi_{13}, \phi_{31}, \phi_{33}$	0.53762

Principal Region of Instability. The boundary frequencies for the first principal region were found for a plate aspect ratio of unity. A step size of $(\Theta/\omega_{11})^2 = 0.005$, where ω_{11} is the smallest natural

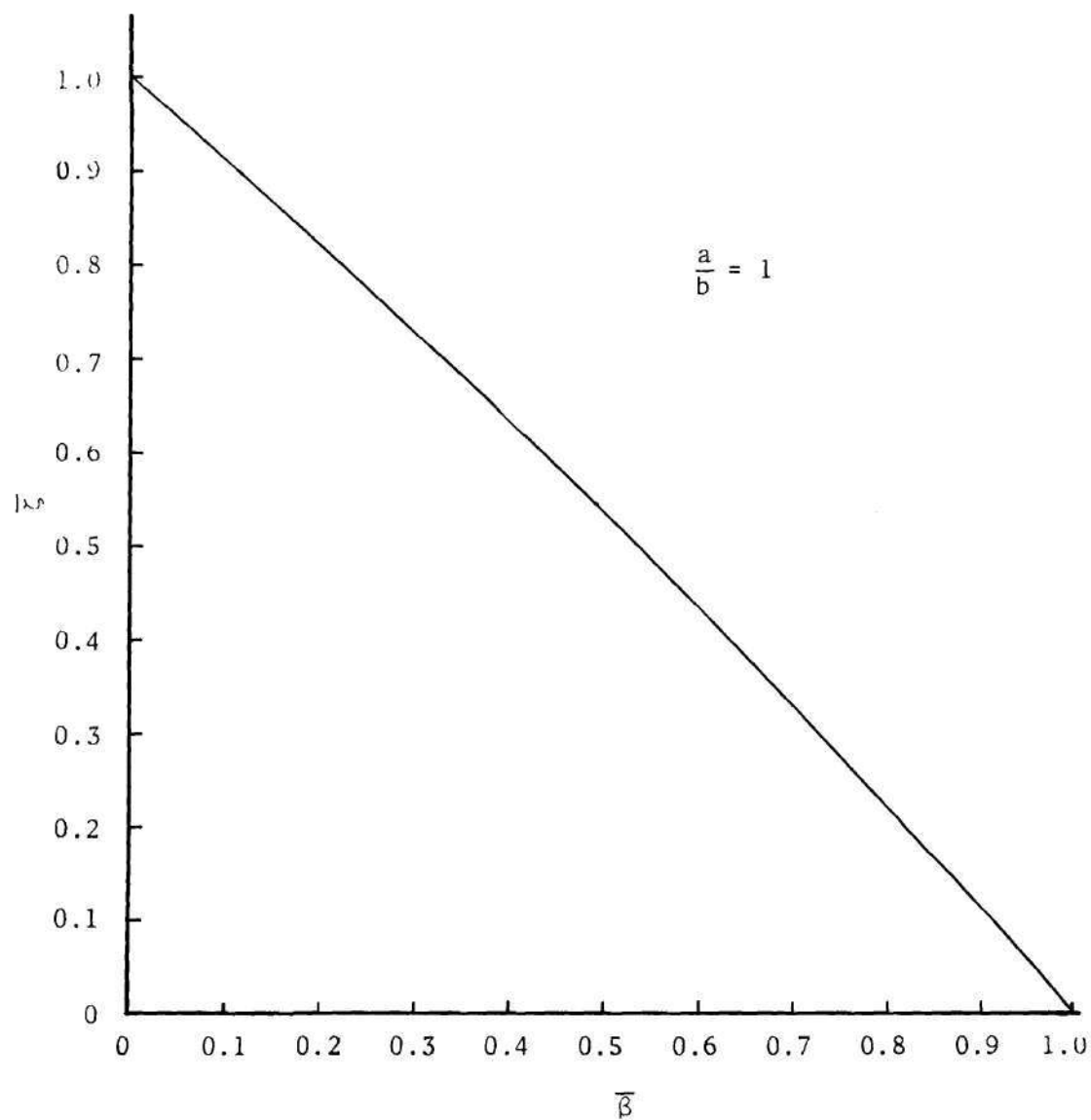


Figure 13. Combination Buckling of Rectangular Plate

frequency of transverse vibration, was used. A range of six values (0, 0.1, 0.2, 0.3, 0.4, 0.5) for each of the parameters $\bar{\zeta}$ and $\bar{\beta}$ was considered.

The four eigenfunctions used in the combination buckling problem were again used. Thus, the matrices appearing in the determinant of Equation (118) were of fourth order. The boundary frequencies were determined from both the first and second order approximations of the infinite determinant. The results for these two approximations were almost identical for small values of $\bar{\beta}$ and $\bar{\zeta}$. For higher values small differences were found. The boundary frequencies obtained from first and second order approximations for upper and lower boundaries are presented in Tables 7 and 8, respectively, for three values of $\bar{\beta}$ and $\bar{\zeta}$. The two entries in each position represent the second and first order approximations, respectively.

The boundaries of the first principal region are plotted in Figure 14 as plots of the excitation frequency ratio, Θ/ω_{11} vs. $\bar{\beta}$, and in Figure 15 as plots of Θ/ω_{11} vs. $\bar{\zeta}$. The plotted points represent the computed values from the second order approximation.

Discussion of Results

Thermal Buckling

The thermal buckling problem was considered primarily to provide a basis for expressing the temperature parameter (ζ) as a ratio. For the circular plate problem the critical temperature parameter was determined for various hot spot diameters. The results plotted in Figure 9 reveal that as the hot spot radius increases from $a = 0.1b$

Table 7. Rectangular Plate--Upper Boundary Frequency $(\theta/\omega_{11})^2$

$\bar{\beta} \backslash \bar{\zeta}$	0.3	0.4	0.5
0.3	3.540, 3.530	3.165, 3.150	2.775, 2.760
0.4	3.745, 3.730	3.370, 3.350	2.985, 2.960
0.5	3.955, 3.930	3.585, 3.550	3.200, 3.160

Table 8. Rectangular Plate--Lower Boundary Frequency $(\theta/\omega_{11})^2$

$\bar{\beta} \backslash \bar{\zeta}$	0.3	0.4	0.5
0.3	2.350, 2.330	1.975, 1.950	1.590, 1.560
0.4	2.165, 2.130	1.795, 1.750	1.420, 1.360
0.5	1.995, 1.930	1.630, 1.550	1.265, 1.160

to $a = 0.9b$ the critical temperature at first decreases and then increases. It is clear that for the hot spot radius zero or equal to the radius of the plate, the thermal stresses vanish, and the plate does not buckle.

Combination Buckling

This problem was considered for two purposes both of which are related to the dynamic stability analysis. The first was to provide a guideline for choosing a set of functions which could adequately represent the plate stiffness properties in the deflection function. The second was to determine the limiting values of $\bar{\beta}$ and $\bar{\zeta}$ below which plate buckling would not occur. Computations for both the

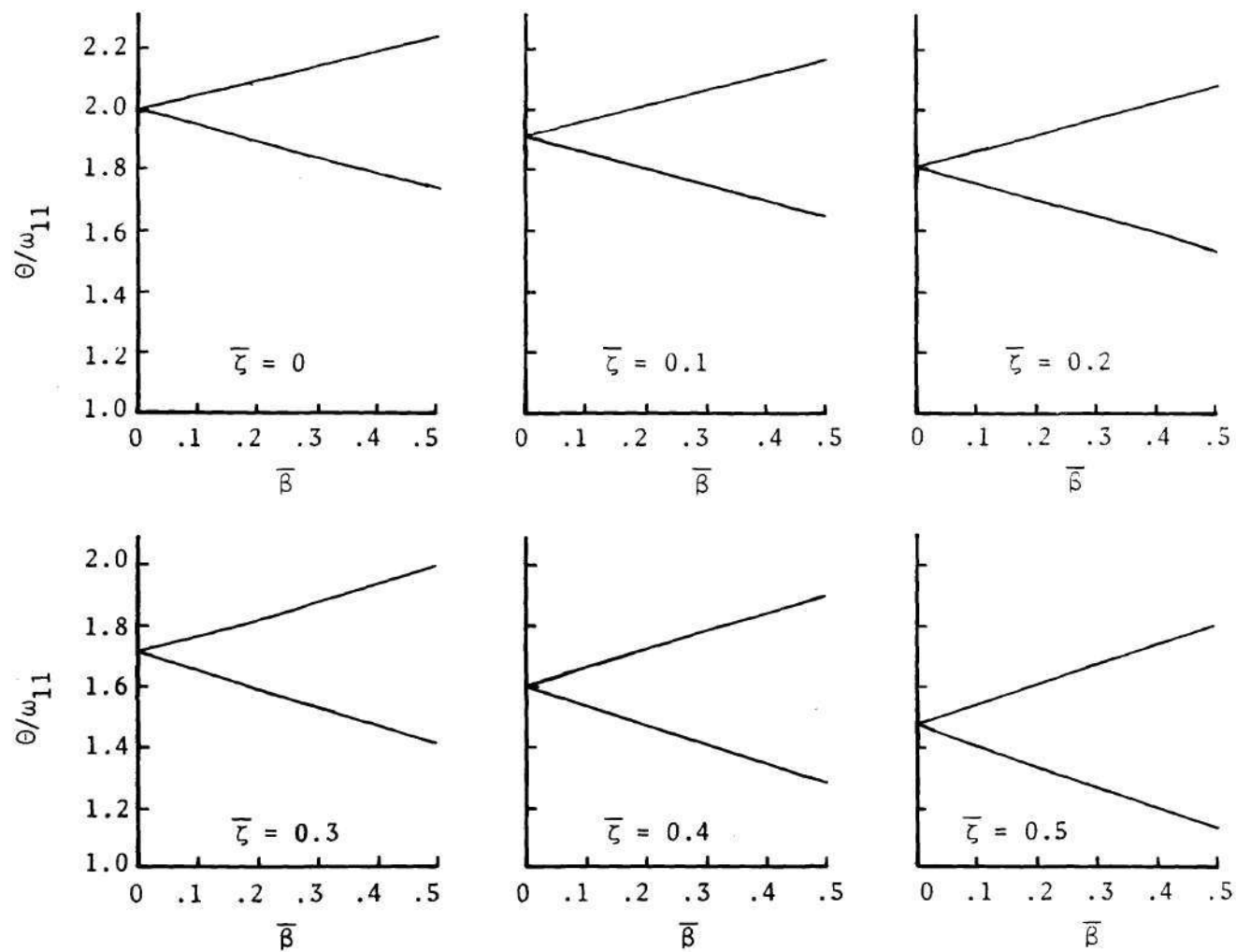


Figure 14. First Principal Region of Instability of the Rectangular Plate.
Excitation Frequency vs. Oscillating Load

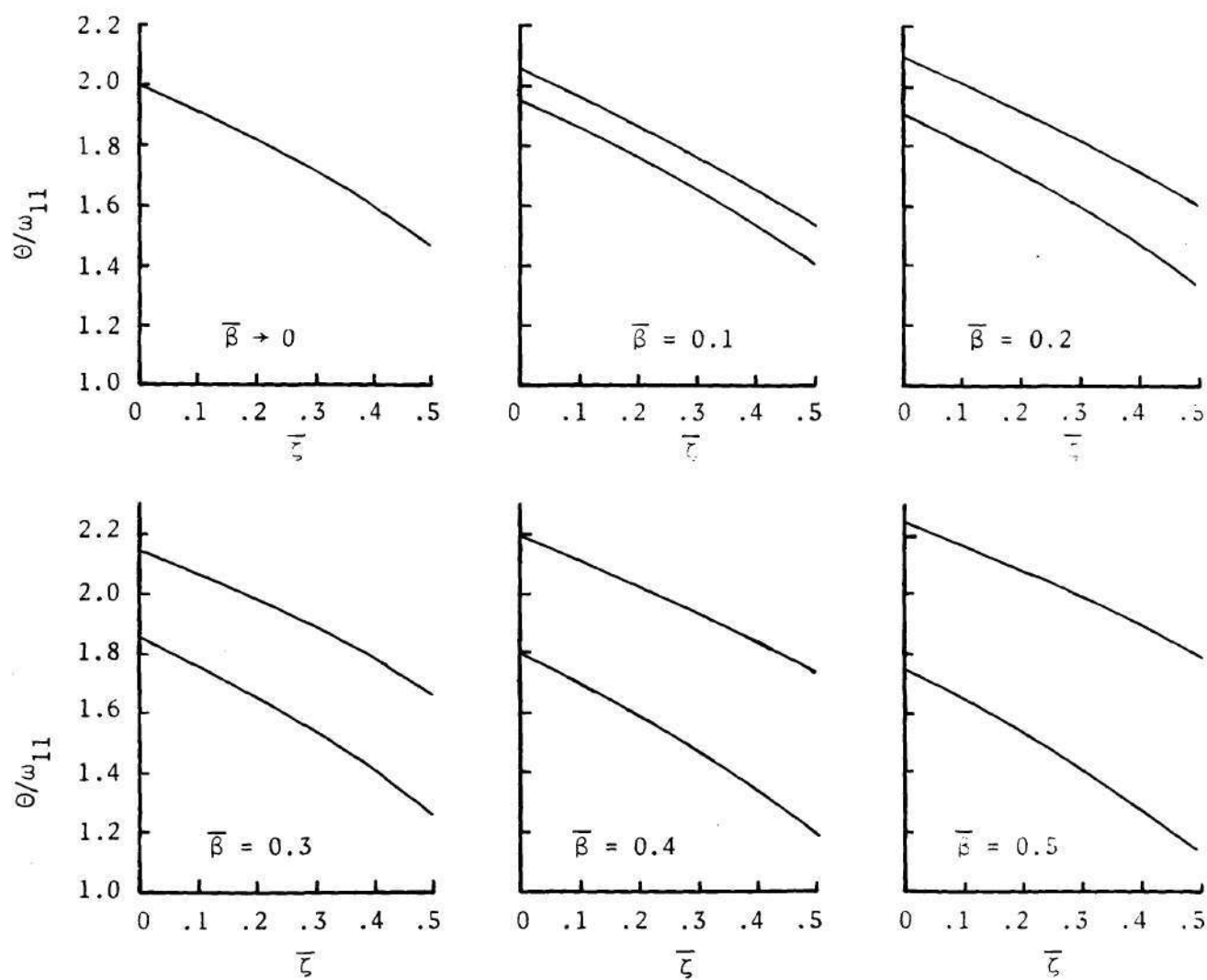


Figure 15. First Principal Region of Instability of the Rectangular Plate.
Excitation Frequency vs. Temperature Parameter

circular and the rectangular plate problems indicated that a set of four functions in the representation of w is adequate.

Dynamic Stability

The first principal region for both the circular and rectangular plates was found for wide ranges of the parameters $\bar{\beta}$ and $\bar{\zeta}$. The scanning procedure used to determine boundary frequencies is convenient because it permits improvement of the accuracy of results for each order of approximation. To obtain the results presented here, a step size was used that produced results well within the accuracy of the plots.

From the plots in Figures 11 and 14 it can be seen that the principal region increases in width as $\bar{\beta}$ increases. Also, from these plots it is found that as $\bar{\zeta}$ increases, these regions cover larger areas. This can be more effectively illustrated by plotting the area of the regions vs. $\bar{\zeta}$. Such a plot is presented in Figure 16. It is found that as $\bar{\zeta}$ increases, while $\bar{\beta}$ covers the same range of values (0 to 0.5), the area of the principal region steadily increases. The increase being about 30 percent as $\bar{\zeta}$ changes from 0.1 to 0.5. Note that the trend is about the same for both the rectangular and circular plates.

The plots in Figures 12 and 15 show that as $\bar{\zeta}$ increases for fixed $\bar{\beta}$, the principal region commences at lower excitation frequencies and curves downward. This behavior is apparently a result of a decrease in effective bending stiffness of the plate as the thermal stresses increase.

It is seen that as $\beta \rightarrow 0$ (Figures 12 and 15) the principal regions

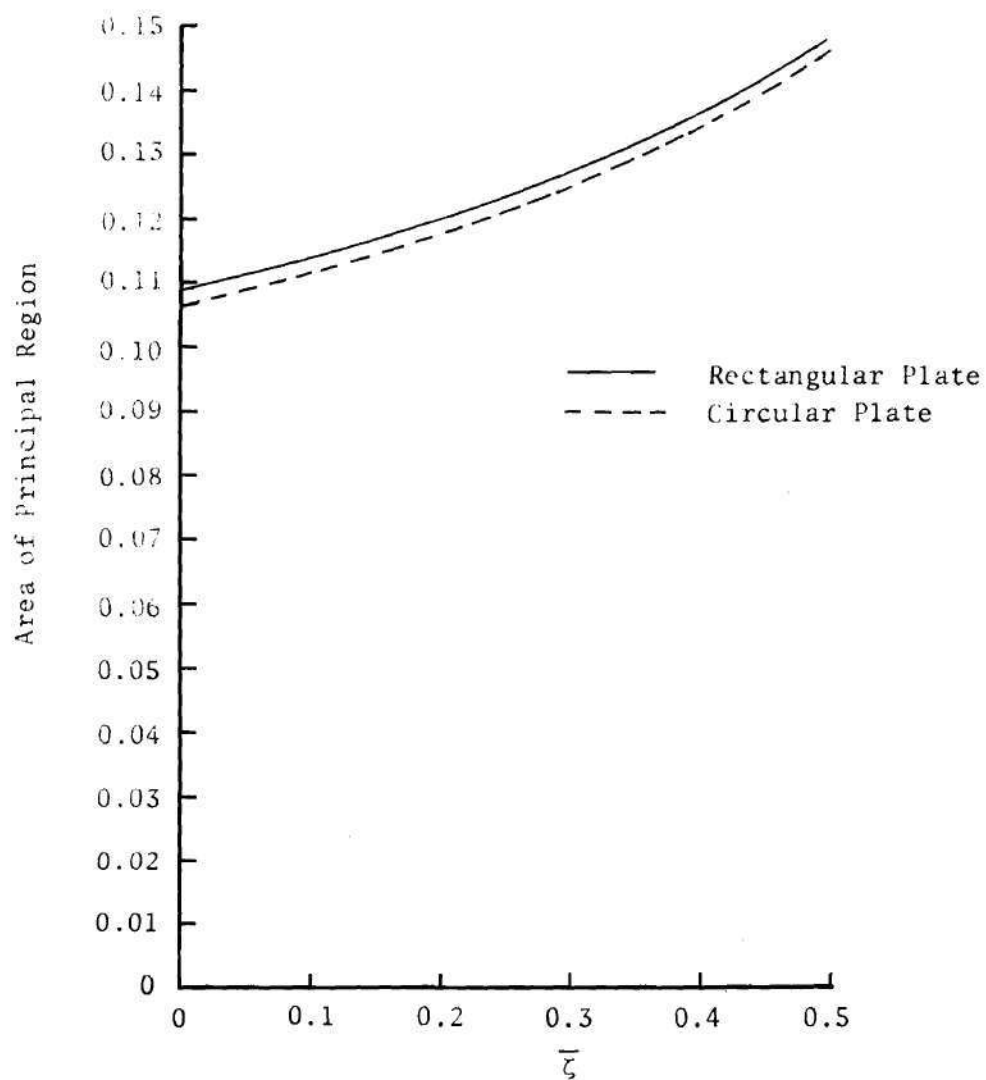


Figure 16. Area of Principal Region vs. Temperature Parameter

degenerate into a line. In fact, as $\beta \rightarrow 0$, Equation (118) for bounding frequencies becomes (note the absence of "+" sign)

$$|\underline{I} - \underline{\zeta E} - \frac{\eta^2 \theta^2}{4} \underline{F}| = 0, \quad \eta = 1, 3, 5, \dots,$$

which yields discrete frequencies instead of ranges of frequencies for which the motion becomes unstable.

The computations of boundary frequencies were carried out for one value of the ratio (a/b) for each of the problems. However, by examining the results presented here some observations may be made about the role of this ratio. In the two unrelated problems it is seen that the principal region, both qualitatively (Figures 11, 12, 14, and 15) and quantitatively (Figure 16), depends on the parameters $\bar{\beta}$ and $\bar{\zeta}$. Thus, for different (a/b) ratios, results similar to those presented here may be expected. It is to be noted, however, a change of (a/b) ratio will change the critical values β_{cr} and ζ_{cr} appearing in Equation (119) which defines $\bar{\beta}$ and $\bar{\zeta}$.

For parametric excitation problems where a static mean stress is present ($\gamma \neq 0$) in addition to the thermal stresses, the effect of thermal stresses may be similar; i.e., the thermal stresses will cause the principal region obtained in the absence of thermal stresses to expand and commence at lower excitation frequencies.

The values of the boundary frequencies determined using the method presented here may not be expected to be realistic for the combinations of $\bar{\beta}$ and $\bar{\zeta}$ which are close to the combination buckling curve (Figures 10 and 13). For such combinations, the effects of

imperfections and middle surface stretching due to bending should be considered. If the system is imperfection insensitive [33], as would be expected for these plate problems, stable configurations can be achieved for loads in excess of the critical values. These configurations are not, however, flat so that the character of the problem differs from those initially posed here.

CHAPTER VI

CONCLUSIONS AND RECOMMENDATIONS FOR FUTURE RESEARCH

Conclusions

Parametric excitation of plates subjected to thermal stresses was studied. The governing equations of motion were derived using the principle of virtual work with reference to a general orthogonal curvilinear coordinate system. An assumed modes approach was used to obtain the equations of motion in terms of generalized coordinates. The development is general and may be used for plates of various shapes with any edge conditions.

The response of the plates to parametric excitation is found to be unstable for some regions of parameters. The boundary frequencies of these regions were shown to be the zeros of infinite determinants. From the results for the first principal region of the two problems considered it was seen that for small amplitude of the oscillating load and small magnitude of thermal stresses, a first order approximation yields satisfactory results. For higher values of these parameters higher order approximations are required.

Thermal effects on the principal region of instability has been investigated for a rectangular and a circular plate. It was found that the regions of instability cover larger areas and commences at lower excitation frequencies as temperature is increased. Thus the presence of thermal stresses reduces the safe operating range of

excitation frequency.

Various values of the amplitude of oscillating load were considered for both the problems. The results show that the principal region widens with increase of the amplitude. As the amplitude tend to zero the region degenerates into a line.

The critical temperature parameter for the circular plate was determined for various values of hot spot radius. It was seen that the critical temperature is smallest for medium size hot spots ($a/b \sim 0.5$). For very small ($a/b \rightarrow 0$) and for large ($a/b \rightarrow 1$) hot spots the critical temperature is very large and thermal buckling is unlikely to occur without the temperature being large enough to alter material properties of the plate.

Recommendations for Future Research

Thermal effects on the dynamic stability of parametrically excited plates has been studied here. For the two plate problems considered the boundaries of the first principal region have been determined. It has been noted earlier that other regions of instability exist. All the analytical results needed to determine these regions have been presented. By carrying out the necessary computations, some of the additional regions may be determined.

To determine the amplitude of the response of the plate within the region of instability, the nonlinear effect of middle surface stretching and the presence of "damping" should be taken into account. To solve such a problem analytically will be difficult, and an experimental investigation may be more appropriate.

Presence of thermal stresses may alter the torsional and

flexural rigidities of beams and arches. This would in turn affect the response of these structures to parametric excitation. These problems should be studied. One simple problem in this line is a simply supported beam subjected to thermal stresses and in-plane parametric excitation.

In the stability analysis (see Chapter III) of parametric excitation response presented here, it was assumed that the eigenvalues ρ_i had multiplicity not greater than two. It is, however, possible that a higher degree of multiplicity may occur. In such cases a phenomenon called combination resonance is observed. The practical importance and significance of this phenomenon needs to be clarified. To this end it is necessary to find out how large the regions of instability are and what frequency ranges they cover. In addition the amplitude of the response in a combination resonance should be determined. This is a mathematically complicated problem and one would be well advised to adopt a combined analytical and experimental approach.

APPENDIX A

STRESS RESULTANTS AND MOMENTS
IN TERMS OF STRAINS

Stress resultants and moments are related to stresses by Equations (14) and (15), respectively. Substituting Equation (6) into Equation (10), and the result in Equations (14) and (15), yields the following expressions for stress resultants and moments in terms of strain components:

$$\begin{aligned} N_{11} &= K(\epsilon_{11} + \nu\epsilon_{22}) - \frac{N^T}{1-\nu} \\ N_{22} &= K(\epsilon_{22} + \nu\epsilon_{11}) - \frac{N^T}{1-\nu} \end{aligned} \quad (A1)$$

$$N_{12} = (1 - \nu)K\epsilon_{12}$$

$$\begin{aligned} M_{11} &= D(\kappa_{11} + \nu\kappa_{22}) - \frac{M^T}{1-\nu} \\ M_{22} &= D(\kappa_{22} + \nu\kappa_{11}) - \frac{M^T}{1-\nu} \end{aligned} \quad (A2)$$

$$M_{12} = (1 - \nu)D\kappa_{12}$$

where

$$N^T = E \int_z e^T dz, \quad M^T = E \int_z e^T dz,$$

and e^T is the thermal strain given by Equation (11). The symbols K and D represent the extensional stiffness

$$K = \frac{Eh}{1 - \nu^2},$$

and the bending stiffness

$$D = \frac{Eh^3}{12(1 - \nu^2)},$$

of the plate. It may be observed here that if the temperature distribution in the plate is symmetric with respect to z , then $M^T = 0$. Stress resultants and moments can be related to displacements by substituting Equations (7) and (8) into Equations (A1) and (A2), respectively. Expressions for vertical shear resultants Q_1 and Q_2 in terms of strain components can be obtained by substituting Equation (A2) into Equation (16).

APPENDIX B

EXISTENCE OF PERIODIC SOLUTIONS

For solutions with period $2\tau(\tau = \frac{2\pi}{\Theta})$, substituting Equation (50) into Equation (48) gives

$$\begin{aligned}
 & - \frac{F}{\eta=1,2} \sum_{\eta=1,2}^{\infty} \frac{\eta^2 \Theta^2}{4} (\phi_{\eta} \sin \frac{\eta \Theta t}{2} + \xi_{\eta} \cos \frac{\eta \Theta t}{2}) \\
 & + (\underline{I} - \gamma \underline{G} - \zeta \underline{E} - \beta \underline{B} \cos \Theta t) [\frac{1}{2} \xi_0 + \sum_{\eta=1,2}^{\infty} (\phi_{\eta} \sin \frac{\eta \Theta t}{2} \\
 & + \xi_{\eta} \cos \frac{\eta \Theta t}{2})] = 0 .
 \end{aligned} \tag{B1}$$

Using some trigonometric identities Equation (B1) becomes

$$\begin{aligned}
 & - \frac{F}{\eta=1,2} \sum_{\eta=1,2}^{\infty} \frac{\eta^2 \Theta^2}{4} (\phi_{\eta} \sin \frac{\eta \Theta t}{2} + \xi_{\eta} \cos \frac{\eta \Theta t}{2}) \\
 & + (\underline{I} - \gamma \underline{G} - \zeta \underline{E}) \sum_{\eta=1,2}^{\infty} (\phi_{\eta} \sin \frac{\eta \Theta t}{2} + \xi_{\eta} \cos \frac{\eta \Theta t}{2}) \\
 & - \frac{\beta}{2} \underline{B} \sum_{\eta=1,2}^{\infty} \phi_{\eta} (\sin \frac{(\eta-2)\Theta t}{2} + \sin \frac{(\eta+2)\Theta t}{2}) \\
 & + \xi_{\eta} (\cos \frac{(\eta-2)\Theta t}{2} + \cos \frac{(\eta+2)\Theta t}{2}) \\
 & + (\underline{I} - \gamma \underline{G} - \zeta \underline{E} - \beta \underline{B} \cos \frac{2\Theta t}{2}) \frac{1}{2} \xi_0 = 0 .
 \end{aligned} \tag{B2}$$

Equating the coefficients of $\sin \frac{\eta \theta t}{2}$ and $\cos \frac{\eta \theta t}{2}$ in Equation (B2), to zero, yields two infinite systems of homogeneous simultaneous equations with unknowns ϕ_{η} and ξ_{η} , respectively. If these equations are arranged such that equations involving odd values of η appear first and then, those involving even values of η (note zero is an even number) and it is required, in each case, that not all the unknowns are zero, the following criterion is obtained:

for ϕ_{η} ,

$$|D_{\text{odd}}|_1 \cdot |D_{\text{even}}|_1 = 0, \quad (\text{B3})$$

for ξ_{η} ,

$$|D_{\text{odd}}|_2 \cdot |D_{\text{even}}|_2 = 0, \quad (\text{B4})$$

where $|D_{\text{odd}}|_1$ and $|D_{\text{odd}}|_2$ are the determinants obtained by taking minus and plus sign, respectively for the "+" sign in the top corner element of the determinant on the left hand side of Equation (51). The determinants $|D_{\text{even}}|_1$ and $|D_{\text{even}}|_2$ are defined by the left hand side of Equations (53) and (52), respectively.

Proceeding similarly, the criteria for existence of solutions of period $\tau (\tau = \frac{2\pi}{\theta})$ are

$$|D_{\text{even}}|_1 = 0, \quad (\text{B5})$$

and

$$|D_{\text{even}}|_2 = 0 . \quad (\text{B6})$$

In view of Equations (B5) and (B6), it is seen that when solutions of period 2τ exists,

$$|D_{\text{even}}|_1 = |D_{\text{even}}|_2 \neq 0 .$$

Consideration of Equations (B3) and (B4) then leads to the condition for existence of solutions of period 2τ ; i.e.,

$$|D_{\text{odd}}|_1 = 0 ,$$

and

$$|D_{\text{odd}}|_2 = 0 .$$

APPENDIX C

INTEGRATION FORMULAE

$$\int_0^r J_m(kr) J_m(lr) r dr = \frac{r}{k^2 - l^2} [kJ_m(lr) J_{m+1}(kr) - lJ_m(kr) J_{m+1}(lr)] \quad (C1)$$

$$\int_0^r I_m(kr) I_m(lr) r dr = \frac{r}{k^2 - l^2} [kI_m(lr) I_{m+1}(kr) - lI_m(kr) I_{m+1}(lr)] \quad (C2)$$

$$\int_0^r I_m(kr) J_m(lr) r dr = \frac{r}{k^2 + l^2} [kJ_m(lr) I_{m+1}(kr) + lI_m(kr) J_{m+1}(lr)] \quad (C3)$$

$$\int_0^r J_m^2(kr) r dr = \frac{r^2}{2} [J_m^2(kr) - J_{m-1}(kr) J_{m+1}(kr)] \quad (C4)$$

$$\int_0^r I_m^2(kr) r dr = \frac{r^2}{2} [I_m^2(kr) - I_{m-1}(kr) I_{m+1}(kr)] \quad (C5)$$

In Equations (C1) through (C5) k and l are constants.

$$\int_0^b \int_0^{2\pi} \phi_{pq}(r, \theta) \nabla^2 \phi_{mn}(r, \theta) r d\theta dr \left\{ \begin{array}{l} = 0, \quad m \neq p \\ = -\epsilon \pi \frac{4\lambda_{mq}^2 \lambda_{mn}^2}{\lambda_{mn}^4 - \lambda_{mq}^4} [\lambda_{mn} J_m(\lambda_{mq}) J_{m+1}(\lambda_{mn}) \\ - \lambda_{mq} J_m(\lambda_{mn}) J_{m+1}(\lambda_{mq})], \quad m = p, n \neq q \\ = -\epsilon \pi \lambda_{mn}^2 [\lambda_{mn} I_{m+1}^2(\lambda_{mn}) \\ + 2m I_m(\lambda_{mn}) I_{m+1}(\lambda_{mn})], \quad m = p, n = q \end{array} \right.$$

The various symbols appearing in this formula are defined in the Circular Plate section of Chapter IV.

APPENDIX D

ELEMENTS OF THE MATRIX E FOR
RECTANGULAR PLATE

$$e_{pqmn} = \frac{D\pi^2}{ab} \{ p [m A_{nq} (B_1 D_{mp} + B_2 E_{mp} + F_{mp}) + n B_{nq} (D_3 G_{mp} + D_4 H_{mp})] \\ + q [n C_{nq} (D_1 I_{mp} + D_2 J_{mp}) + m B_{qn} (D_3 G_{pm} + D_4 H_{pm})] \}$$

The constants B_1 , B_2 and D_1 through D_4 are given by

$$B_1 = \frac{k_1 \sinh R_1 \cos R_2 - k_2 \cosh R_1 \sin R_2}{k_1 \sin R_2 \cos R_2 + k_2 \sinh R_1 \cosh R_1}$$

$$B_2 = - \frac{k_1 \cosh R_1 \sin R_2 + k_2 \sinh R_1 \cos R_2}{k_1 \sin R_2 \cos R_2 + k_2 \sinh R_1 \cosh R_1}$$

$$D_1 = B_1(k_1^2 - k_2^2) - 2B_2k_1k_2$$

$$D_2 = B_2(k_1^2 - k_2^2) + 2B_1k_1k_2$$

$$D_3 = B_1k_2 + B_2k_1$$

$$D_4 = B_1k_1 - B_2k_2$$

where

$$R_1 = k_1 \frac{a}{b}$$

$$R_2 = k_2 \frac{a}{b}$$

$$k_1 = 4 \sqrt{\frac{105}{13}} \sqrt{1 + \sqrt{\frac{21}{65}}}$$

$$k_2 = 4 \sqrt{\frac{105}{13}} \sqrt{1 - \sqrt{\frac{21}{65}}}$$

The other coefficients are

$$A_{nq} = - \frac{1}{\left(\frac{n-q}{2} \pi\right)^2} \quad \text{if } \left|\frac{n-q}{2}\right| \text{ is odd}$$

$$= - \frac{1}{\left(\frac{n+q}{2} \pi\right)^2} \quad \text{if } \left|\frac{n-q}{2}\right| \text{ is even or zero}$$

$$B_{nq} = \frac{a/b}{\left(\frac{n-q}{2} \pi\right)^3} \quad \text{if } \left|\frac{n-q}{2}\right| \text{ is odd}$$

$$= \frac{a/b}{\left(\frac{n+q}{2} \pi\right)^3} \quad \text{if } \left|\frac{n-q}{2}\right| \text{ is even or zero}$$

$$C_{nq} = \left(\frac{a}{b}\right)^2 \frac{1}{\left(\frac{n-q}{2} \pi\right)^4} \quad \text{if } \left|\frac{n-q}{2}\right| \text{ is odd}$$

$$= - \left(\frac{a}{b}\right)^2 \frac{1}{\left(\frac{n+q}{2} \pi\right)^4} \quad \text{if } \left|\frac{n-q}{2}\right| \text{ is even}$$

$$= \left(\frac{a}{b}\right)^2 \left[\frac{1}{48} - \frac{1}{\left(\frac{n+q}{2} \pi\right)^4} \right] \text{ if } n = q$$

$$D_{mp} = (-1)^{\frac{m-p}{2} + 1} [(C_1 + C_2 + C_3 + C_4) \sinh R_1 \cos R_2 \\ - (C_5 + C_6 + C_7 + C_8) \cosh R_1 \sin R_2]$$

$$E_{mp} = (-1)^{\frac{m-p}{2}} [(C_1 + C_2 + C_3 + C_4) \cosh R_1 \sin R_2 \\ + (C_5 + C_6 + C_7 + C_8) \sinh R_1 \cos R_2]$$

$$F_{mp} = \begin{cases} 0 & \text{if } m \neq p \\ \frac{1}{2} & \text{if } m = p \end{cases}$$

$$G_{mp} = (-1)^{\frac{m-p}{2}} [(C_1 - C_2 + C_3 - C_4) \sinh R_1 \cos R_2 \\ - (C_5 - C_6 + C_7 - C_8) \cosh R_1 \sin R_2]$$

$$H_{mp} = (-1)^{\frac{m-p}{2}} [(C_1 - C_2 + C_3 - C_4) \cosh R_1 \sin R_2 \\ + (C_5 - C_6 + C_7 - C_8) \sinh R_1 \cos R_2]$$

$$I_{mp} = (-1)^{\frac{m-p}{2}} [(C_1 + C_2 - C_3 - C_4) \sinh R_1 \cos R_2 \\ - (C_5 + C_6 - C_7 - C_8) \cosh R_1 \sin R_2]$$

$$J_{mp} = (-1)^{\frac{m-p}{2} + 1} [(C_1 + C_2 - C_3 - C_4) \cosh R_1 \sin R_2 \\ + (C_5 + C_6 - C_7 - C_8) \sinh R_1 \cos R_2]$$

where

$$C_1 = \frac{1}{4} \frac{R_2 + \frac{m+p}{2} \pi}{R_1^2 + (R_2 + \frac{m+p}{2} \pi)^2}$$

$$C_2 = \frac{1}{4} \frac{R_2 - \frac{m+p}{2} \pi}{R_1^2 + (R_2 - \frac{m+p}{2} \pi)^2}$$

$$C_3 = \frac{1}{4} \frac{R_2 + \frac{m-p}{2} \pi}{R_1^2 + (R_2 + \frac{m-p}{2} \pi)^2}$$

$$C_4 = \frac{1}{4} \frac{R_2 - \frac{m-p}{2} \pi}{R_1^2 + (R_2 - \frac{m-p}{2} \pi)^2}$$

$$C_5 = \frac{1}{4} \frac{R_1}{R_1^2 + (R_2 + \frac{m+p}{2} \pi)^2}$$

$$C_6 = \frac{1}{4} \frac{R_1}{R_1^2 + (R_2 - \frac{m+p}{2} \pi)^2}$$

$$C_7 = \frac{1}{4} \frac{R_1}{R_1^2 + (R_2 + \frac{m-p}{2} \pi)^2}$$

$$C_8 = \frac{1}{4} \frac{R_1}{R_1^2 + (R_2 - \frac{m-p}{2} \pi)^2}$$

REFERENCES

1. Beliaev, N. M., "Stability of Prismatic Rods Subjected to Variable Longitudinal Forces," Engineering Constructions and Structural Mechanics, Leningrad, Russia, 1924, p. 149.
2. Einaudi, R., "About Unstable Equilibrium States of Plates Subject to Periodic Shear Stresses," *Atti Accad. Gioenia, Memoria XX*, 1935, p. 1.
3. Chelomei, V. N., "Dynamic Stability of Plates," *Tr. Kiev. Aviats. Inst.*, No. 10, 1938.
4. Bodner, V. A., "Stability of Plates Subjected to Longitudinal Periodic Forces," *Prikl. Mat. i Mekhan.*, Vol. 2, No. 1, 1938, p. 87.
5. Bolotin, V. V., The Dynamic Stability of Elastic Systems, Holden-Day, San Francisco, California, 1964.
6. Carlson, R. L., "An Experimental Study of the Parametric Excitation of a Tensioned Sheet with a Cracklike Opening," *Experimental Mechanics*, Vol. 14, No. 11, Nov. 1974, p. 452.
7. Beilin, E. A. and Dzhanelidze, G. U., "Survey of Work on the Dynamic Stability of Elastic Systems," *Prikl. Mat. i Mekhan.*, Vol. 16, No. 5, p. 635.
8. Evan-Iwanowski, R. M., "On the Parametric Response of Structures," *Applied Mechanics Review*, Vol. 18, No. 9, Sept. 1965, p. 699.
9. Duhamel, J. M. C., "Mémoire sur le calcul des actions moléculaires développées par les changements de température dans les corps solides," *Mémoires par divers savants*, Vol. 5, 1838, p. 440 (The paper was read before the Academy of Sciences on February 23, 1835).
10. Boley, B. A. and Weiner, J. H., Theory of Thermal Stresses, John Wiley, New York, 1960.
11. Gatewood, B. E., Thermal Stresses, McGraw-Hill, New York, 1957.
12. Nowacki, W., Thermoelasticity, Pergamon, London, 1962.
13. van der Neut, A., "Buckling Caused by Thermal Stresses," *AGRADograph 28*, Pergamon Press, London, 1958.
14. Gossard, M. L. et al., "Thermal Buckling of Plates," NACA TN 2771, 1952.

15. Boley, B. A., "Thermally Induced Vibrations of Beams," J. of the Aero. Sciences, Vol. 23, No. 2, February 1956, p. 179.
16. Boley, B. A. and Barber, A. D., "Dynamic Response of Beams and Plates to Rapid Heating," J. of Appl. Mech., Vol. 24, No. 3, September 1957, p. 413.
17. Sun, C. L. and Lu, S. V., "Nonlinear Dynamic Behavior of Heated Conical and Cylindrical Shells," Nuclear Engineering and Design, Vol. 7, North-Holland, Amsterdam, Holland, 1968, p. 113.
18. Novozhilov, V. V., Foundation of the Nonlinear Theory of Elasticity, Graylock, Rochester, New York, 1953.
19. Jakob, M., Heat Transfer, John Wiley, New York, Vol. I, 1949, Vol. II, 1957.
20. Washizu, K., Variational Methods in Elasticity and Plasticity, Pergamon, London, 1968.
21. Rektorys, K. (ed.), Survey of Applicable Mathematics, MIT Press, Cambridge, Massachusetts, 1969, p. 819.
22. Wylie, C. R., Advanced Engineering Mathematics, McGraw-Hill, New York, 1966, p. 495.
23. Meirovitch, L., Methods of Analytical Dynamics, McGraw-Hill, New York, 1970.
24. Bolotin, V. V., loc. cit., Ref. 6, p. 215.
25. Meirovitch, L., loc. cit., Ref. 23, p. 268.
26. Parkes, E. W., "Stresses in a Plate due to a Local Hot Spot," Aircraft Engineering, Vol. 29, No. 3, March 1957, p. 67.
27. Meirovitch, L., Analytical Methods in Vibrations, Macmillan, London, 1967, p. 179.
28. Reid, W. P., "Free Vibrations of a Circular Plate," J. Soc. Ind. Appl. Math., Vol. 10, No. 4, December 1962, p. 668.
29. Heldenfels, R. R. and Roberts, W. M., "Experimental and Theoretical Determination of Thermal Stresses in a Flat Plate," NACA TN 2769, August 1952.
30. Kantorovich, L. V. and Krylov, V. I., Approximate Methods of Higher Analysis, John Wiley, New York, 1964, p. 304.
31. Timoshenko, S. P. and Gere, J. M., Theory of Elastic Stability, McGraw-Hill, New York, 1961.

32. Meirovitch, L., loc. cit., Ref. 27, p. 91.
33. Croll, J. G. and Walker, A. C., Elements of Structural Stability, John Wiley, New York, 1972, p. 91.

VITA

Parthasarathi Mukhopadhyay was born on August 20, 1948 in Abadanga, West Bengal (India), to Shiba Prasad and Kamala Mukhopadhyay. He attended Bankura Zilla School, graduating in 1964. He earned his B. Tech. at the Indian Institute of Technology, Kharagpur and his M. Eng. at the Asian Institute of Technology, Bangkok (Thailand). In the fall of 1972 he joined Georgia Institute of Technology as a graduate student and research assistant in the School of Aerospace Engineering.